Figure 1

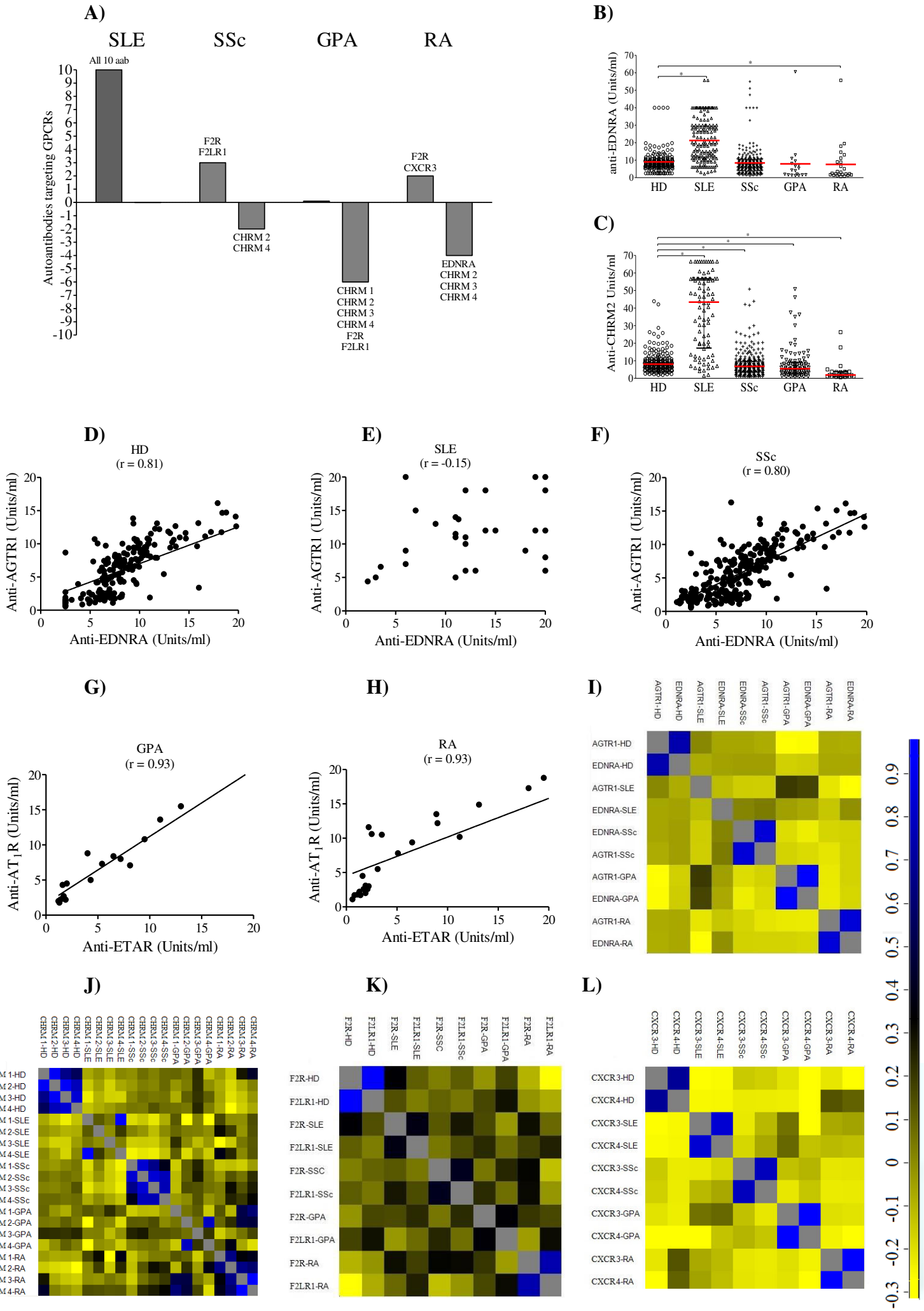
A)
SLE
SSc
GPA
RA
All 10 aab
F2R F2LR1
CHRM 2 CHRM 4
F2R CXCR3
CHRM 1 CHRM 2 CHRM 3 CHRM 4 F2R F2LR1
EDNRA CHRM 2 CHRM 3 CHRM 4
Autoantibodies targeting GPCRs
B)
anti-EDNRA (Units/ml)
HD
SLE
SSc
GPA
RA
C)
Anti-CHRM2 Units/ml
D)
HD
(r = 0.81)
Anti-AGTR1 (Units/ml)
Anti-EDNRA (Units/ml)
E)
SLE
(r = -0.15)
F)
SSc
(r = 0.80)
G)
GPA
(r = 0.93)
Anti-AT1R (Units/ml)
Anti-ETAR (Units/ml)
H)
RA
(r = 0.93)
I)
AGTR1-HD
EDNRA-HD
AGTR1-SLE
EDNRA-SLE
EDNRA-SSc
AGTR1-SSc
AGTR1-GPA
EDNRA-GPA
AGTR1-RA
EDNRA-RA
J)
CHRM 1-HD
CHRM 2-HD
CHRM 3-HD
CHRM 4-HD
CHRM 1-SLE
CHRM 2-SLE
CHRM 3-SLE
CHRM 4-SLE
CHRM 1-SSc
CHRM 2-SSc
CHRM 3-SSc
CHRM 4-SSc
CHRM 1-GPA
CHRM 2-GPA
CHRM 3-GPA
CHRM 4-GPA
CHRM 1-RA
CHRM 2-RA
CHRM 3-RA
CHRM 4-RA
K)
F2R-HD
F2LR1-HD
F2R-SLE
F2LR1-SLE
F2R-SSC
F2LR1-SSc
F2R-GPA
F2LR1-GPA
F2R-RA
F2LR1-RA
L)
CXCR3-HD
CXCR4-HD
CXCR3-SLE
CXCR4-SLE
CXCR3-SSc
CXCR4-SSc
CXCR3-GPA
CXCR4-GPA
CXCR3-RA
CXCR4-RA

Figure 1. Relationships among autoantibodies in healthy donors and patients with systemic autoimmune diseases. **A**) The graphic summarizes anti-GPCR aab in healthy donor (HD), which showed concentrations significantly increased or decreased when compared to the disease cohorts (systemic lupus erythematosus or SLE, systemic sclerosis or SSc, granulomatosis with polyangiitis or GPA, and rheumatoid arthritis or RA). Further details are shown in **Supplementary Figure 1**. The x axis represents healthy controls. Graphics display concentrations of aab directed against **B**) EDNRA and **C**) CHRM2. Linear regression graphics exhibit the correlation between anti-EDNRA and anti-AGTR1 aab in sera from **D**) HD, **E**) SLE, **F**) SSc, **G**) GPA, and **H**) RA. Heatmaps of autoantibody *versus* autoantibody correlations demonstrate the spectrum of relationships between aab targeting **I**) EDNRA and AGTR1; **J**) CHRMs; **K**) F2R and FLR1; **L**) CXCR3 and CXCR4 (for nomenclature, see **Supplementary Table 2,** *aab dataset 1*). The bar ranging from yellow to blue represents negative to positive correlations, respectively. In the correlation matrix, each small square represents a pairwise correlation between aab as exemplified by D-H. The correlation matrices used to perform the hierarchical correlograms shown in Fig 1I-L are provided as Source data.

Figure 2

A)

HD – cohort 1

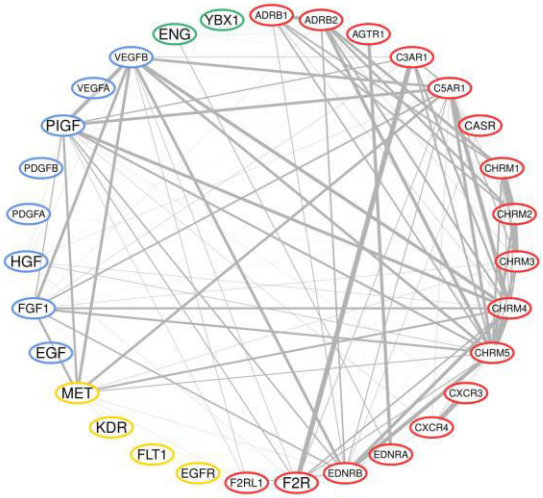

B)

SSc

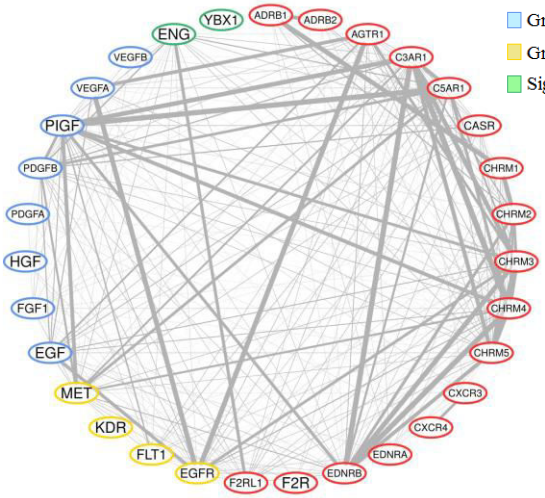

C)

Females

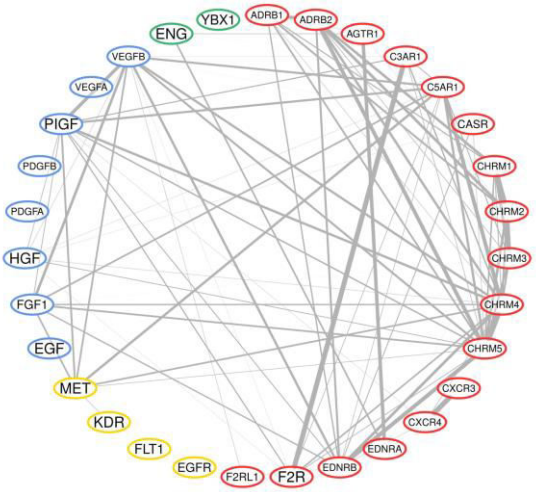

D)

Males

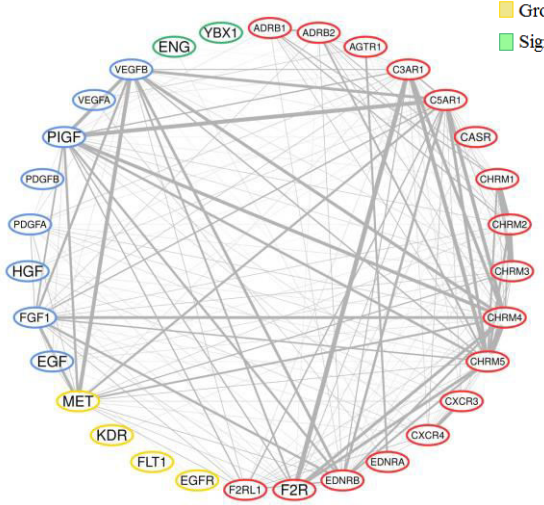

E)

<65

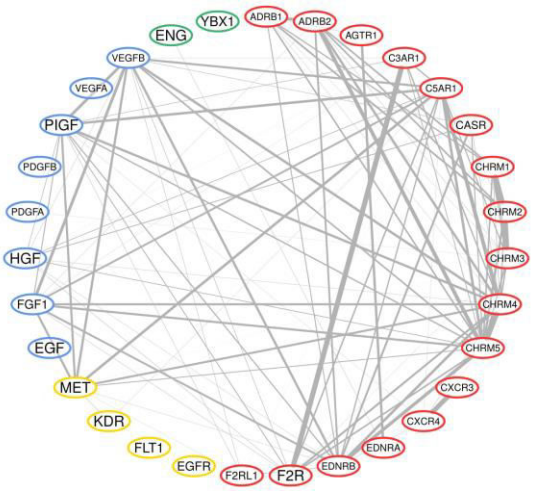

F)

≥65

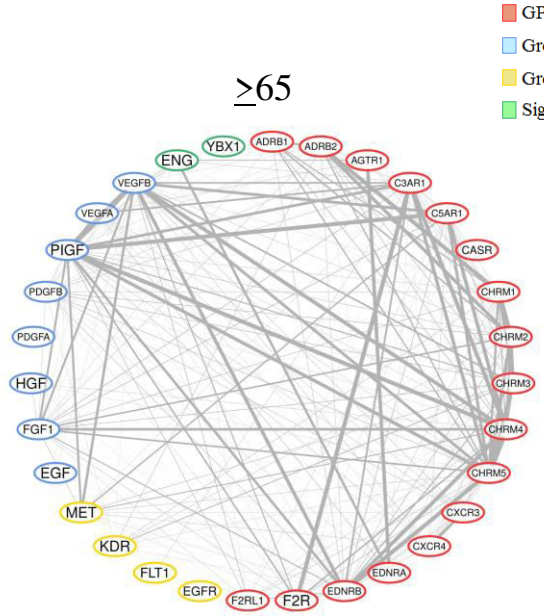

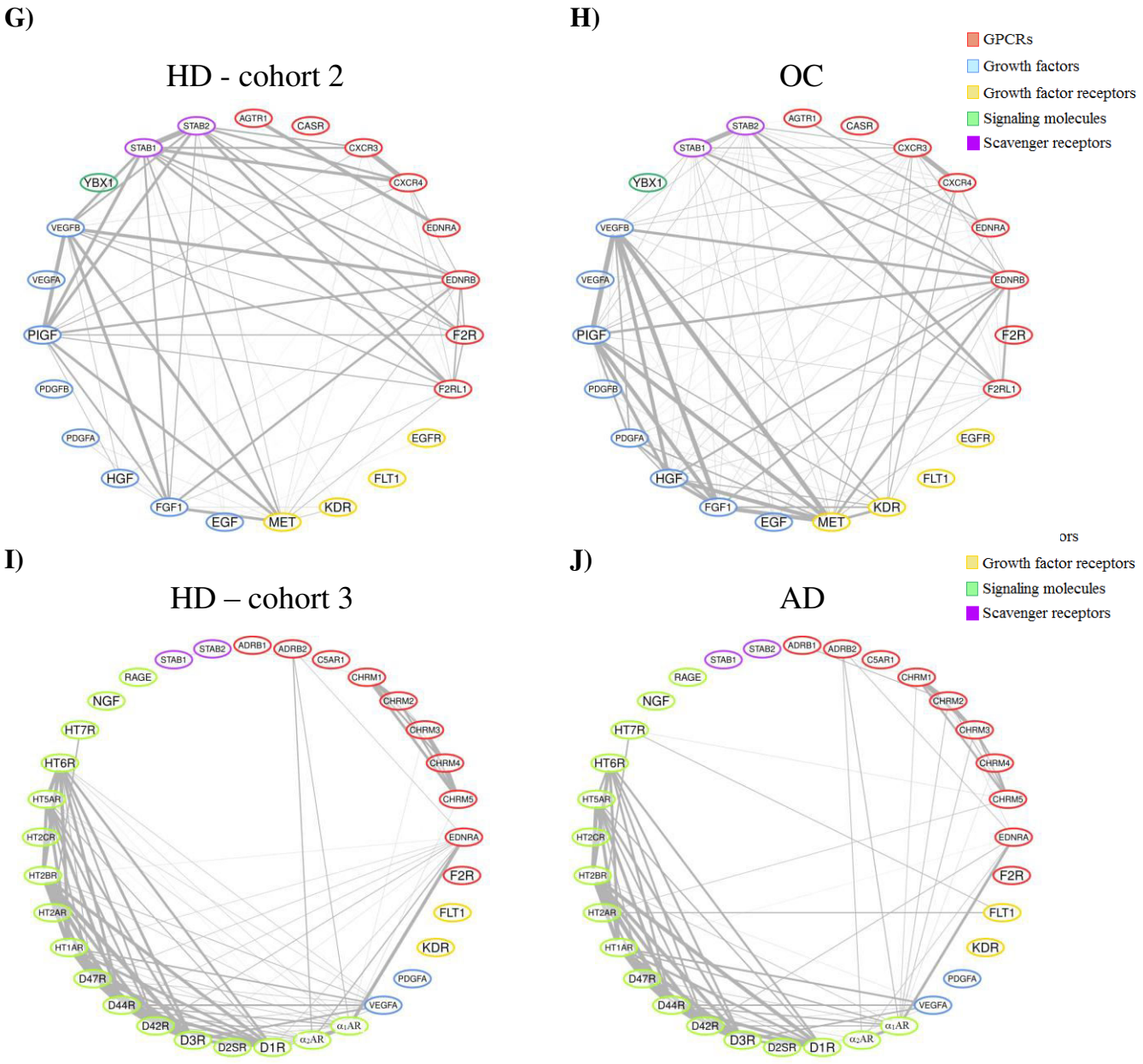

Figure 2. Effects of gender, age and disease on the correlations between aab. We analyzed the relationships between the different aab in sera from HD and the effects of gender and age as shown by circular networks based on aab Spearman's rank correlation coefficients. Circle plots show the correlation matrix of aab, comparing each condition: **A**) all healthy donors (HD) evaluated, **B**) patients with systemic sclerosis (SSc; **Supplementary Table 1,** *Cohort 1*; **Supplementary Table 2,** *aab dataset 1*); subgroups of HD (*Cohort 1*) analyzed according to **C-D**) gender and **E-F**) age (< and ≥ 65 years). Graphics also display comparison between **G**) HD and patients with **H**) ovarian cancer (OC; **Supplementary Table 1,** *Cohort 2*; **Supplementary Table 2,** *aab dataset 2*), and **I**) HD and patients with **J**) Alzheimer's disease (AD; **Supplementary Table 1,** *Cohort 3*; **Supplementary Table 2,** *aab dataset 3*). The nodes in the graphs represent variables (each aab) and a line between two nodes indicates the Spearman's rank correlation coefficient. Line width indicates the strength of association, stronger correlations leading to thicker lines. Only correlations >0.6 are shown. Multiple connections between nodes indicate clustering.

Figure 3

A)

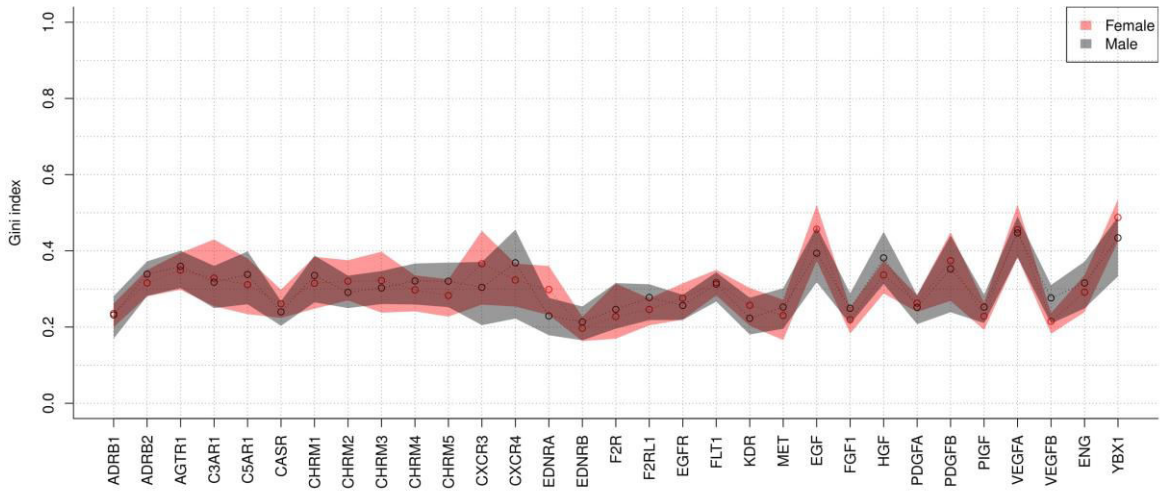
Female
Male
Gini index
0.0
0.2
0.4
0.6
0.8
1.0
ADRB1
ADRB2
AGTR1
C3AR1
C5AR1
CASR
CHRM1
CHRM2
CHRM3
CHRM4
CHRM5
CXCR3
CXCR4
EDNRA
EDNRB
F2R
F2RL1
EGFR
FLT1
KDR
MET
EGF
FGF1
HGF
PDGFA
PDGFB
PIGF
VEGFA
VEGFB
ENG
YBX1

B)

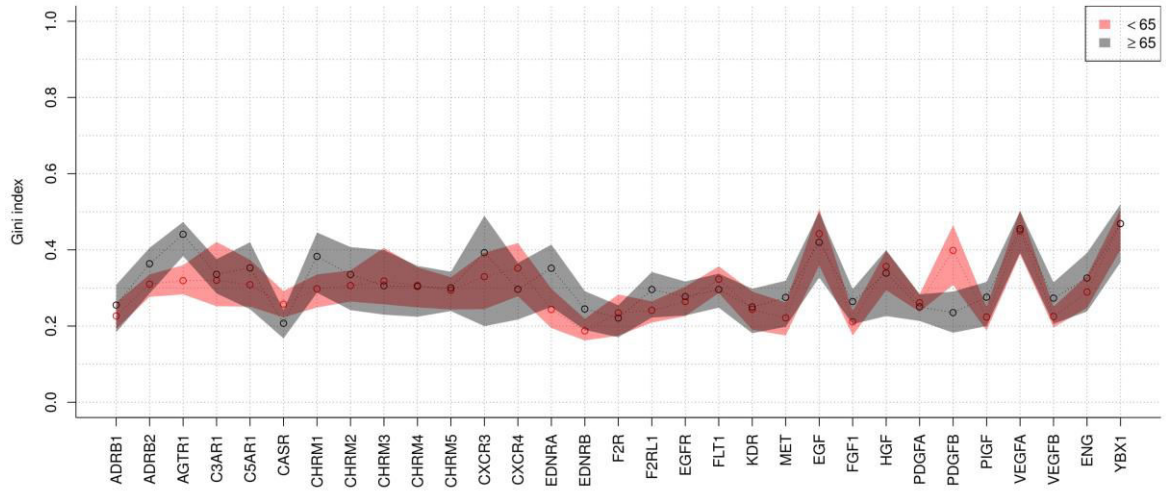
< 65
≥ 65
Gini index
0.0
0.2
0.4
0.6
0.8
1.0
ADRB1
ADRB2
AGTR1
C3AR1
C5AR1
CASR
CHRM1
CHRM2
CHRM3
CHRM4
CHRM5
CXCR3
CXCR4
EDNRA
EDNRB
F2R
F2RL1
EGFR
FLT1
KDR
MET
EGF
FGF1
HGF
PDGFA
PDGFB
PIGF
VEGFA
VEGFB
ENG
YBX1

C)

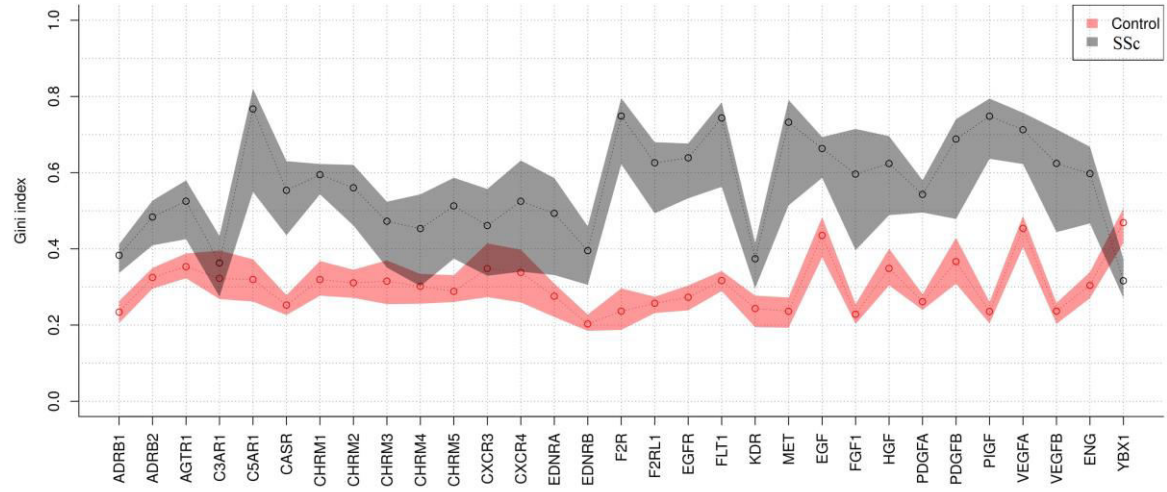
Control
SSc
Gini index
0.0
0.2
0.4
0.6
0.8
1.0
ADRB1
ADRB2
AGTR1
C3AR1
C5AR1
CASR
CHRM1
CHRM2
CHRM3
CHRM4
CHRM5
CXCR3
CXCR4
EDNRA
EDNRB
F2R
F2RL1
EGFR
FLT1
KDR
MET
EGF
FGF1
HGF
PDGFA
PDGFB
PIGF
VEGFA
VEGFB
ENG
YBX1

D)

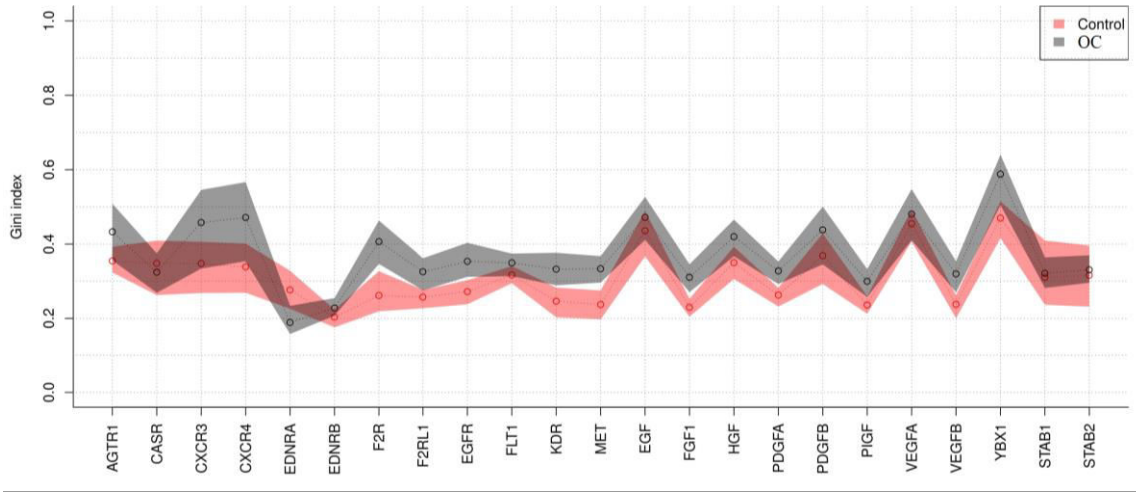

E)

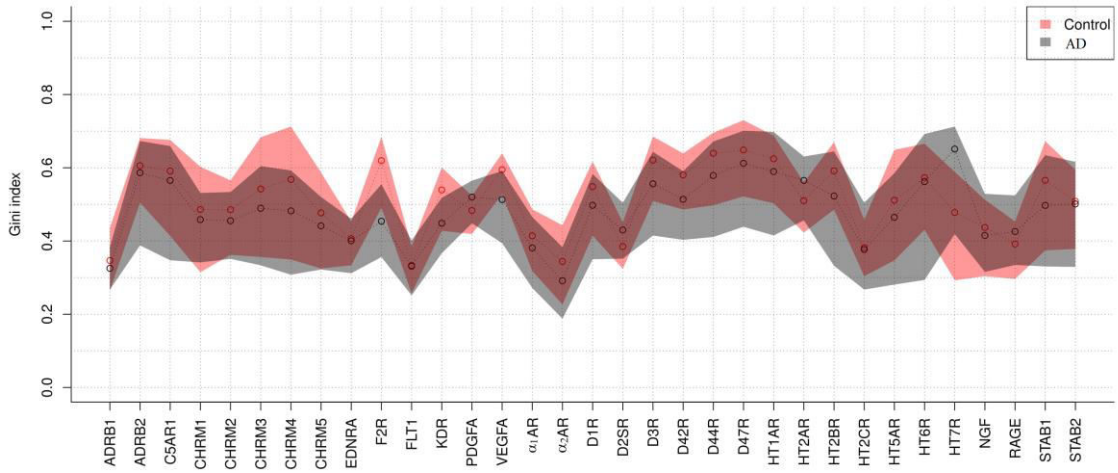

Figure 3. Aab relationships reflect the distribution patterns of aab concentrations. Gini index confidence intervals were obtained by bootstrap analysis. The red and grey shadows represent confidence intervals and each small circle indicates the Gini index value. The graphics exhibit comparisons between **A)** HD females and males, **B)** HD above and below 65 years (**Supplementary Tab 1,** *Cohort 1*; **Supplementary Table 2,** *aab dataset 1*). Comparisons between **C**) HD and patients with systemic sclerosis (SSc, **Supplementary Table 1,** *Cohort 1*; **Supplementary Table 2,** *aab dataset 1*, **D**) HD and patients with ovarian cancer (OC, **Supplementary Table 1,** *Cohort 2*; **Supplementary Table 2,** *aab dataset 2*), or **E**) HD and patients with Alzheimer's disease (AD, **Supplementary Table 1,** *Cohort 3*; **Supplementary Table 2,** *aab dataset 3*).

Figure 4

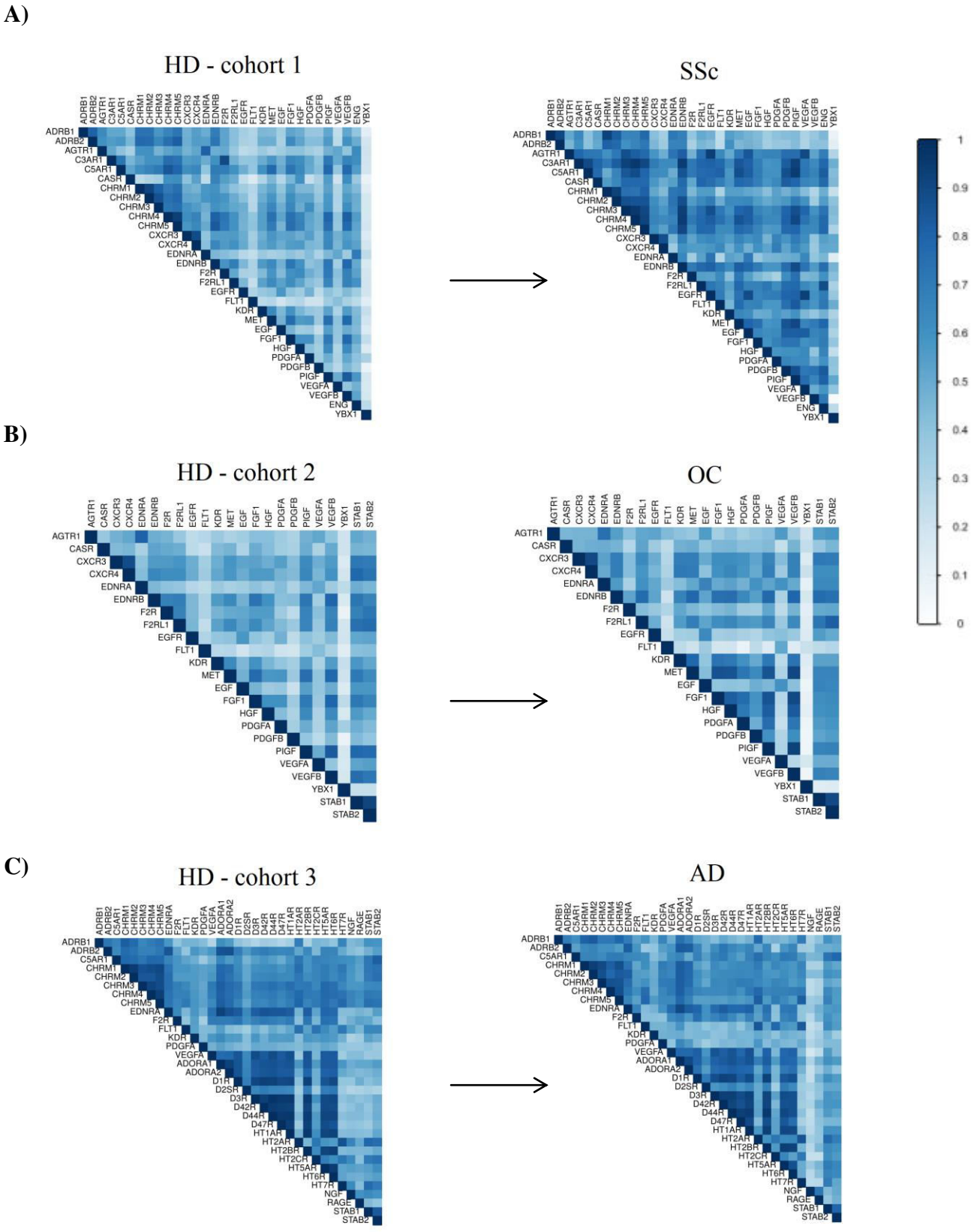

Figure 4. Heatmaps of autoantibody correlations. The images exhibit Spearman´s correlation of autoantibody (aab) datasets (**Supplementary Table 2**) **A)** 1, **B)** 2 and **C)** 3 in sera from the healthy donors (HD) cohorts 1 – 3 and patients (systemic sclerosis, SSc; ovarian cancer**,** OC; and Alzheimer's disease, AD), respectively (**Supplementary Table 1**). A correlation spectrum from 0 to 1, corresponding to weak and strong correlation, is shown.

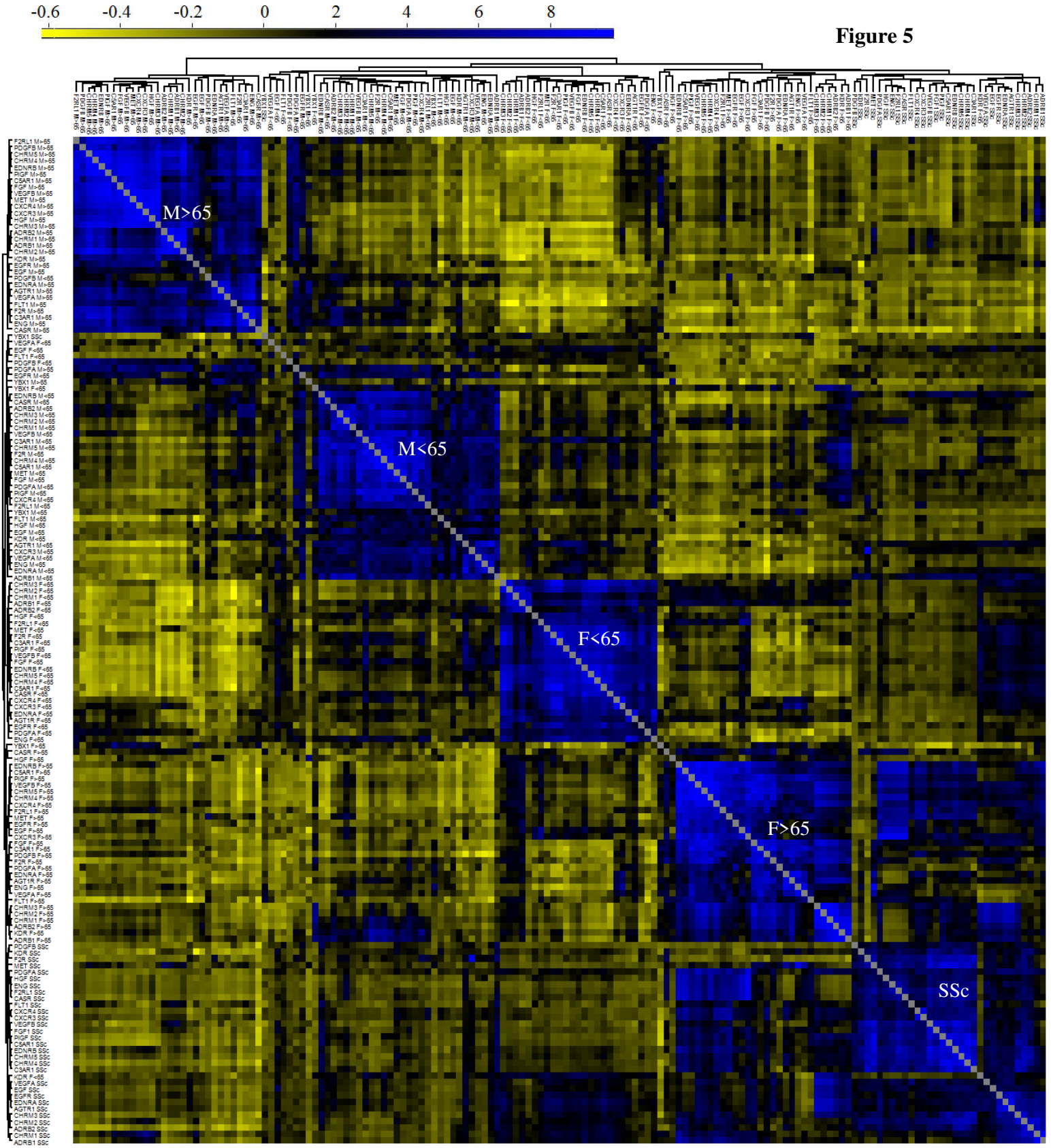

Figure 5

Figure 5. Hierarchical clustering analysis reveals correlation signatures of autoantibodies according to gender, age and disease. Correlogram matrix displays clusters (modules) of autoantibody (aab) correlations in all healthy donors (HD) according to gender and age (< and ≥65 years) compared to patients with systemic sclerosis (SSc; **Supplementary Tab 1,** *Cohort 1*; **Supplementary Table 2,** *aab dataset 1*). Clusters of correlation between aab are displayed in dendrograms on the top and the side of the correlation matrix. The bar ranging from yellow to blue represents negative to positive correlations, respectively. In the heat map matrix, each small square represents the pairwise correlations between aab. The correlation matrix used to perform the hierarchical correlogram of SSc is provided as Source data.

Figure 6

A)

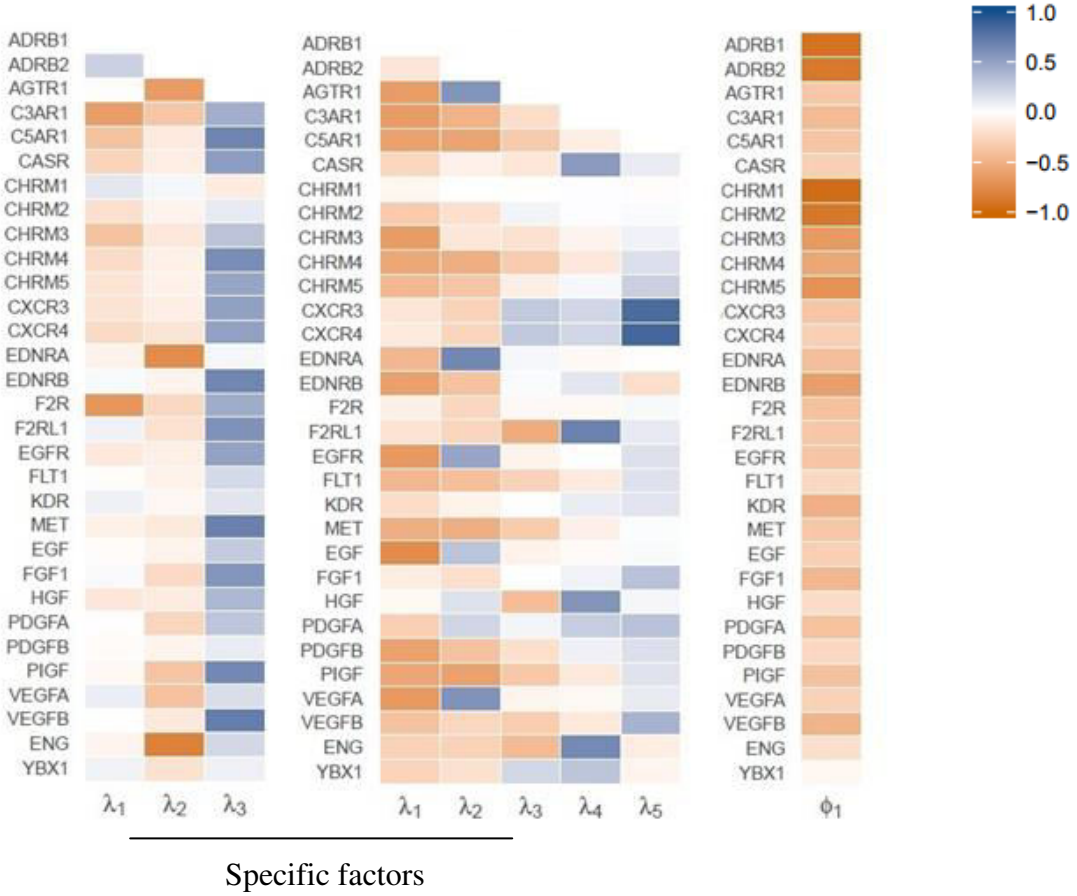
Controls
SSc
Shared factor
1.0
0.5
0.0
−0.5
−1.0
ADRB1
ADRB2
AGTR1
C3AR1
C5AR1
CASR
CHRM1
CHRM2
CHRM3
CHRM4
CHRM5
CXCR3
CXCR4
EDNRA
EDNRB
F2R
F2RL1
EGFR
FLT1
KDR
MET
EGF
FGF1
HGF
PDGFA
PDGFB
PIGF
VEGFA
VEGFB
ENG
YBX1
λ1 λ2 λ3
λ1 λ2 λ3 λ4 λ5
ϕ1
Specific factors

B)

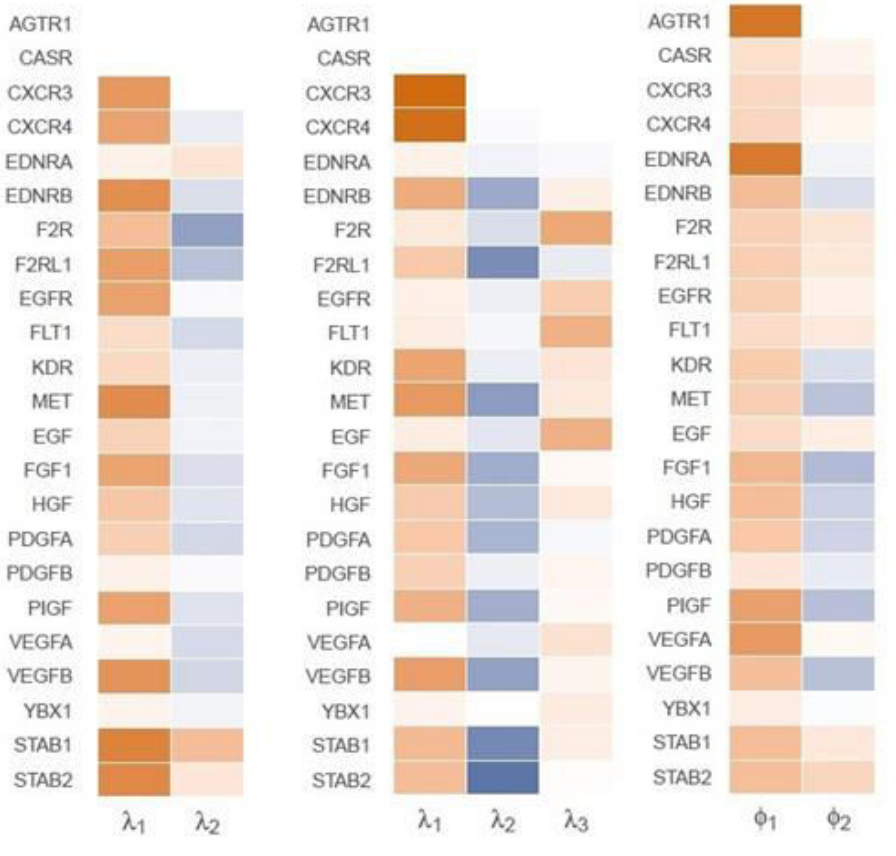
Controls
OC
Shared factors
AGTR1
CASR
CXCR3
CXCR4
EDNRA
EDNRB
F2R
F2RL1
EGFR
FLT1
KDR
MET
EGF
FGF1
HGF
PDGFA
PDGFB
PIGF
VEGFA
VEGFB
YBX1
STAB1
STAB2
λ1 λ2
λ1 λ2 λ3
ϕ1 ϕ2
Specific factors

C)

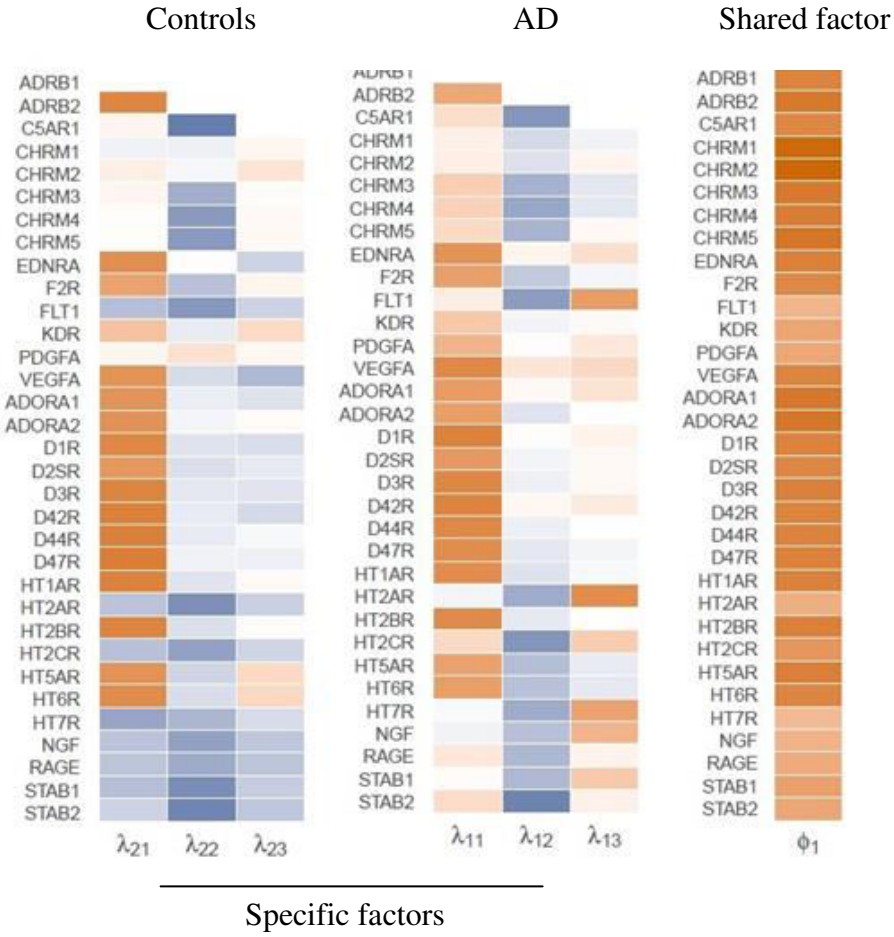

Figure 6. Multi-study factor analysis of aab. The multi-study factor analysis (MSFA) was performed to analyze aab from healthy donors (HD) and compare to patients with **A**) systemic sclerosis (SSc), **B**) ovarian cancer (OC), and **C)** Alzheimer's disease (AD). **Supplementary tables 1 and 2** provide further details about HD and patient groups, as well as aab datasets analyzed. The images are heatmaps of estimated factor loadings of common and specific latent factors. Loadings close to 1 or -1 indicate aab that strongly influence factors in opposite directions.

Figure 7

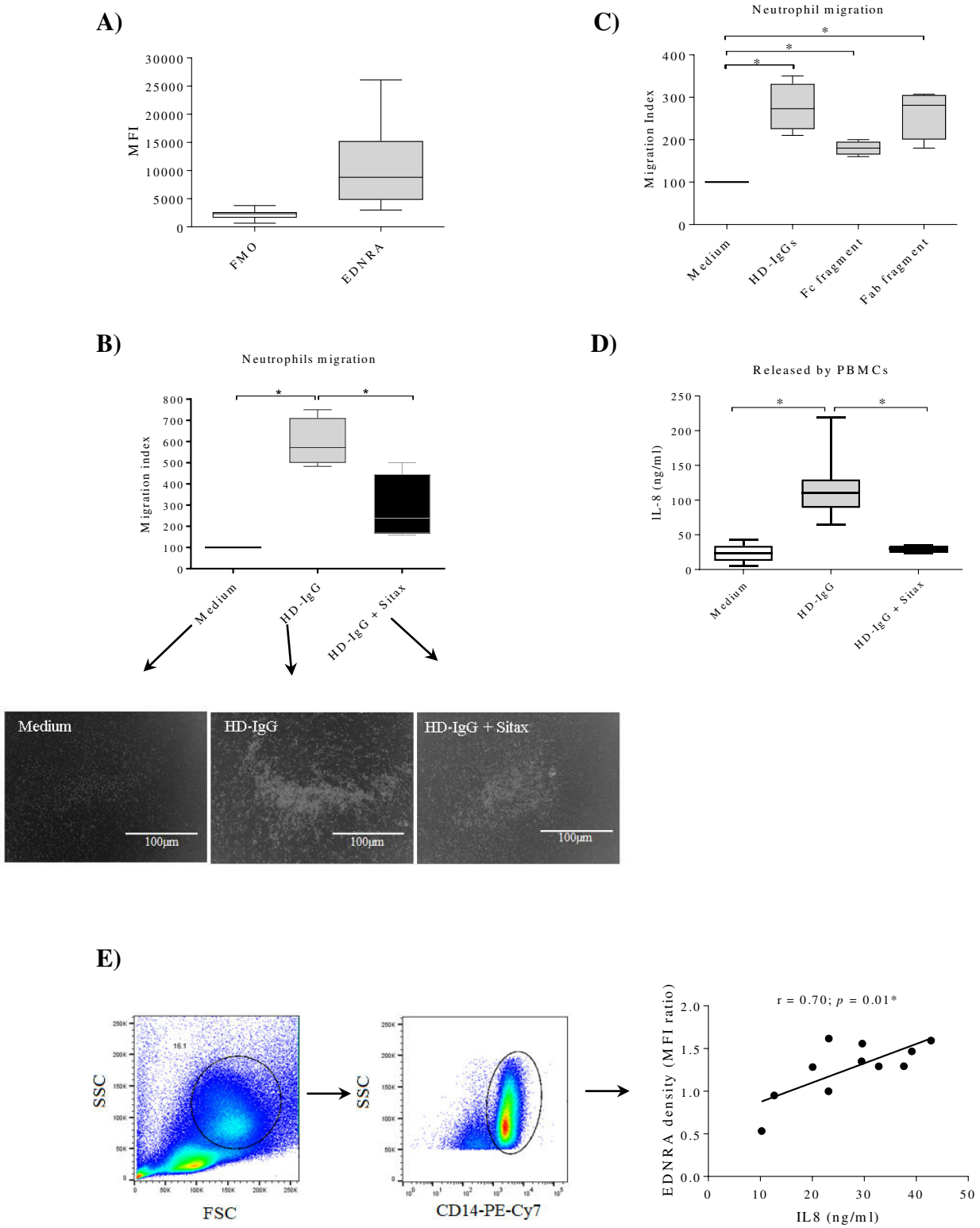
A)
MFI
30000
25000
20000
15000
10000
5000
0
FMO
EDNRA
C)
Neutrophil migration
Migration Index
400
300
200
100
0
Medium
HD-IgGs
Fc fragment
Fab fragment
B)
Neutrophils migration
Migration index
800
700
600
500
400
300
200
100
0
Medium
HD-IgG
HD-IgG + Sitax
D)
Released by PBMCs
IL-8 (ng/ml)
250
200
150
100
50
0
Medium
HD-IgG
HD-IgG + Sitax
Medium
HD-IgG
HD-IgG + Sitax
100µm
E)
SSC
FSC
CD14-PE-Cy7
r = 0.70; p = 0.01*
EDNRA density (MFI ratio)
IL8 (ng/ml)

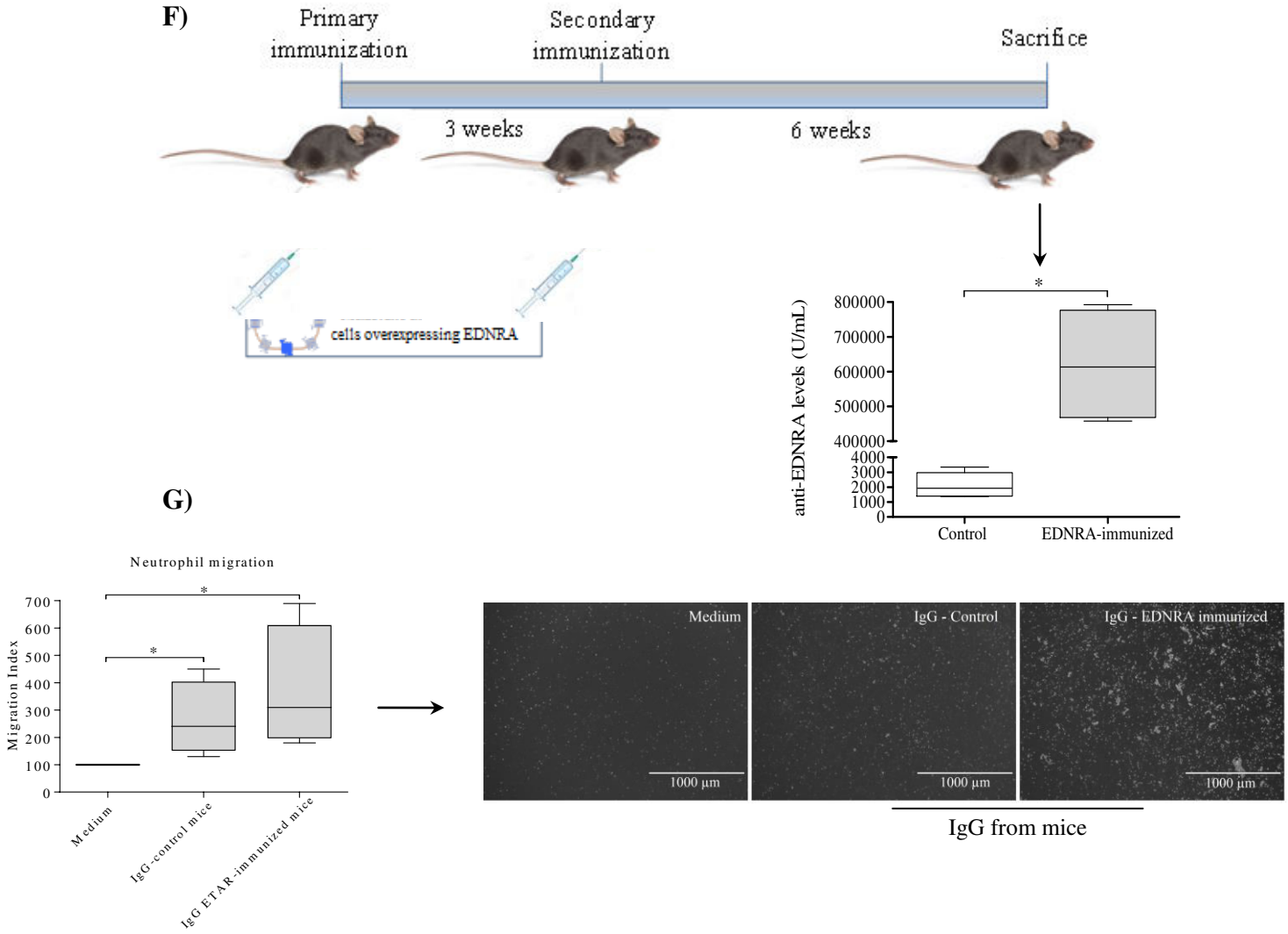

Figure 7. Effect of HD-IgG and anti-EDNRA antibodies on migration of neutrophils and their distribution throughout the host. A) Expression of endothelin receptor type A (EDNRA) by human neutrophils. The fluorescence minus one control (FMO) was analyzed as shown in **Supplementary Figure 5. B**) Neutrophil chemotaxis toward 0.5 mg/ml IgG from healthy donors (HD-IgG) was analyzed by transwell migration assay in the presence or absence of the EDNRA antagonist sitaxsentan (sitax). A representative image of neutrophils (white dots in the figure) on bottom surface of transwell plates is shown. The migration index was calculated in relation to the spontaneous (medium) migration (index 100) **C**) Neutrophil migration towards intact human IgG, antigen-binding fragment (Fab), and the crystallized fragment (Fc) region. The results are representative of three independent experiments (n = 3). **D**) 0.5 mg/ml HD-IgG induced IL-8 production by peripheral blood mononuclear cells (PBMCs) after 24 hours stimulation in an EDNRA dependent-manner as demonstrated by the inhibition of IL-8 production in the presence of sitaxsentan. **E**) The level of IL-8 spontaneously released into the culture supernatants correlates with the level of EDNRA expression on CD14+ monocytes. IL-8 concentration was assessed by ELISA and EDNRA expression analyzed by flow cytometry (n = 11). Significant differences are denoted by asterisk when $p \leq 0.05$ (Mann-Whitney test). **F**) Concentrations of anti-EDNRA aab in mouse sera were assessed after secondary immunization with membrane extracts from control Chinese hamster ovary (CHO) cells or CHO cells overexpressing human EDNRA (n = 5). EDNRA-immunization was carried out given into footpads 0.2 mg of membrane extracts prepared from CHO cells overexpressing human EDNRA (Celltrend, Germany). Three weeks after the primary immunization, mice were boosted

with the same amount of membrane emulsified with incomplete Freund adjuvant (IFA, Sigma-Aldrich, USA). In the control group, mice were treated with the same amount of membrane extract from untransfected CHO cells. Six weeks after booster immunization, all mice were sacrificed for sample collection and quantification of anti-EDNRA aab. **G**) Migration of human neutrophils (white dots in the figure) toward IgG from control and EDNRA-immunized mice (n = 3).

Supplementary Table 1

HD (cohort 1)	*<65*	*≥65*	*total*	*Mean Age*
male	42	24	66	60.3 ± 7.8
female	104	23	127	57.6 ± 7.2
total	146	47	193	58.5 ± 7.5
Systemic Sclerosis	*<65*	*≥65*	*total*	*Mean Age*
male	1	13	14	52.8 ± 9.4
female	62	8	70	56.9 ± 13
total	63	21	84	56.2 ± 12.5

HD (cohort 2)	*<65*	*≥65*	*total*	*Mean Age*
male	43	23	66	60.4 ± 7.9
female	104	25	129	57.7 ± 7.1
total	147	48	195	58.9 ± 7.5
Ovarian cancer	*<65*	*≥65*	*total*	*Mean Age*
male	0	0	0	0
female	141	66	207	59.1 ± 11.4
total	141	66	207	59.1 ± 11.4

HD (cohort 3)	*<65*	*≥65*	*total*	*Mean Age*
male	1	26	27	73.9 ± 6.5
female	11	65	76	72.5 ± 8.6
total	12	91	103	73.5 ± 7.5
Alzheimer´s disease	*<65*	*≥65*	*total*	*Mean Age*
male	4	21	25	73.4 ± 7.9
female	5	61	66	75.8 ± 7.4
total	9	82	91	74.9 ± 7.8

Supplementary Table 1. Demographics of healthy donors and patients. All healthy donors (HD) are German subjects not receiving medications known to have any effect on the immune response. Three different HD cohorts, cohort 1 (upper panel), cohort 2 (middle panel) and cohort 3 (lower panel) were used throughout the study for comparison with patients affected by systemic sclerosis (SSc), ovarian cancer (OC) and Alzheimer's disease (AD)**,** respectively.

Supplementary Table 2

Aab dataset 1 – HD (cohort 1) and SSc	Full Name
G protein-coupled receptors	
AT1R or *AGTR1*	angiotensin II receptor type 1
ADRB1	beta-1 adrenergic receptor
ADRB2	beta-2 adrenergic receptor
CASR	calcium-sensing receptor
CXCR3	chemokine (C-X-C) motif receptor 3
CXCR4	chemokine (C-X-C) motif receptor 4
C3AR1	complement component 3a receptor 1
C5AR1	complement component 5a receptor 1
ETAR or *EDNRA*	endothelin receptor type A
ETBR *EDNRB*	endothelin receptor type B
M1 or *CHRM1*	cholinergic receptor muscarinic 1
M2 or *CHRM2*	cholinergic receptor muscarinic 2
M3 or *CHRM3*	cholinergic receptor muscarinic 3
M4 or *CHRM4*	cholinergic receptor muscarinic 4
M5 or *CHRM5*	cholinergic receptor muscarinic 5
PAR1 or *F2R*	Protease-activated receptor 1
PAR2 or *F2RL1*	Protease-activated receptor 2
Growth factors	
EGF	epidermal growth factor
FGF1	fibroblast growth factor 1
HGF	hepatocyte growth factor
PDGFA	platelet-derived growth factor alpha
PDGFB	platelet-derived growth factor beta
VEGFA	vascular endothelial growth factor A
VEGFB	vascular endothelial growth factor B
PIGF	Placental growth factor
Growth factor receptors	
EGFR	epidermal growth factor receptor
HGFR or *MET*	hepatocyte growth factor receptor
VEGFR1 or *FLT1*	vascular endothelial growth factor 1
VEGFR2 or *KDR*	vascular endothelial growth factor 2
Signaling molecules	
YBX1	Y-box-binding protein 1
ENG	Endoglin

Aab dataset 2 - HD (cohort 2) and OC	Full Name
G protein-coupled receptors	
AT1R or *AGTR1*	angiotensin II receptor type 1
CASR	calcium-sensing receptor
CXCR3	chemokine (C-X-C) motif receptor 3
CXCR4	chemokine (C-X-C) motif receptor 4
ETAR or *EDNRA*	endothelin receptor type A
ETBR *EDNRB*	endothelin receptor type B
PAR1 or *F2R*	Protease-activated receptor 1
PAR2 or *F2RL1*	Protease-activated receptor 2
Growth factor receptors	
EGF	epidermal growth factor
FGF1	fibroblast growth factor
HGF	hepatocyte growth factor
PDGFA	platelet-derived growth factor alpha
PDGFB	platelet-derived growth factor beta
VEGFA	vascular endothelial growth factor A
VEGFB	vascular endothelial growth factor B
PIGF	Placental growth factor
Growth factor receptors	
EGFR	epidermal growth factor receptor
HGFR or *MET*	hepatocyte growth factor receptor
VEGFR1 or *FLT1*	vascular endothelial growth factor 1
VEGFR2 or *KDR*	vascular endothelial growth factor 2
Signaling molecules	
YBX1	Y-box-binding protein 1
Scavenger receptors	
STAB1	Stabilin-1
STAB2	Stabilin-2

Aab dataset 3 – HD (cohort 3) and AD	Full Name
G protein-coupled receptors	
ADRB1	beta-1 adrenergic receptor
ADRB2	beta-2 adrenergic receptor
C5AR1	complement component 5a receptor 1
ETAR or *EDNRA*	endothelin receptor type A
M1 or *CHRM1*	cholinergic receptor muscarinic 1
M2 or *CHRM2*	cholinergic receptor muscarinic 2
M3 or *CHRM3*	cholinergic receptor muscarinic 3
M4 or *CHRM4*	cholinergic receptor muscarinic 4
M5 or *CHRM5*	cholinergic receptor muscarinic 5
PAR1 or *F2R*	Protease-activated receptor 1
Growth factors	
PDGFA	platelet-derived growth factor alpha polypeptide
VEGFA	vascular endothelial growth factor A
Growth factor receptors	
VEGFR1 or *FLT1*	vascular endothelial growth factor 1
VEGFR2 or *KDR*	vascular endothelial growth factor 2
Neurological or AD-associated Molecules	
α_1AR	Alpha 1 adrenoceptor
α2AR	Alpha 2 adrenoceptor
D1R	D1 Dopamine receptor
D2SR	D2s Dopamine receptor
D3R	D3 Dopamine receptor
D42R	D42 Dopamine receptor
D44R	D44 Dopamine receptor
D47R	D47 Dopamine receptor
HT1AR	5-hydroxytryptamine receptor 1
HT2AR	5-hydroxytryptamine receptor 2A
HT2BR	5-hydroxytryptamine receptor 2B
HT2CR	5-hydroxytryptamine receptor 2C
HT5AR	5-hydroxytryptamine receptor 5
HT6R	5-hydroxytryptamine receptor 6
HT7R	5-hydroxytryptamine receptor 7
NGF	Nerve growth factor beta
RAGE	Receptor for advanced glycation end products
Signaling molecules	
YBX1	Y-box-binding protein 1
ENG	Endoglin
Scavenger receptors	
STAB1	Stabilin-1
STAB2	Stabilin-2

Supplementary Table 2. **Autoantibody datasets.** Three datasets of autoantibodies (aab) were analyzed in sera from three healthy donor (HD) cohorts and patients with systemic sclerosis (SSc, upper left panel) ovarian cancer (OC, lower left panel) and patients with Alzheimer's disease (AD, upper right panel).

Supplementary Table 3

Antibodies			
Antibody targets	*Fluorochrome*	*Clone or number*	*Manufacturer*
CD14	PE-Cy7/Alexa Fluor 647	HCD14/ M5E2	Biolegend
CD15	Brillant Violet 510	W6D3	Biolegend
Anti-Rabbit IgG	CFL405	Sc-362252	SantaCruz
Anti-Rabbit IgG	Brillant Violet 421	Poly4064	Biolegend
EDNRA	n.a.	sc-33535	Santa Cruz
Isotype 1	n.a.	sc-3888	Santa Cruz

Supplementary Table 3. Antibody panel used for the flow cytometric analyses of EDNRA expression.

Supplementary Figure 1

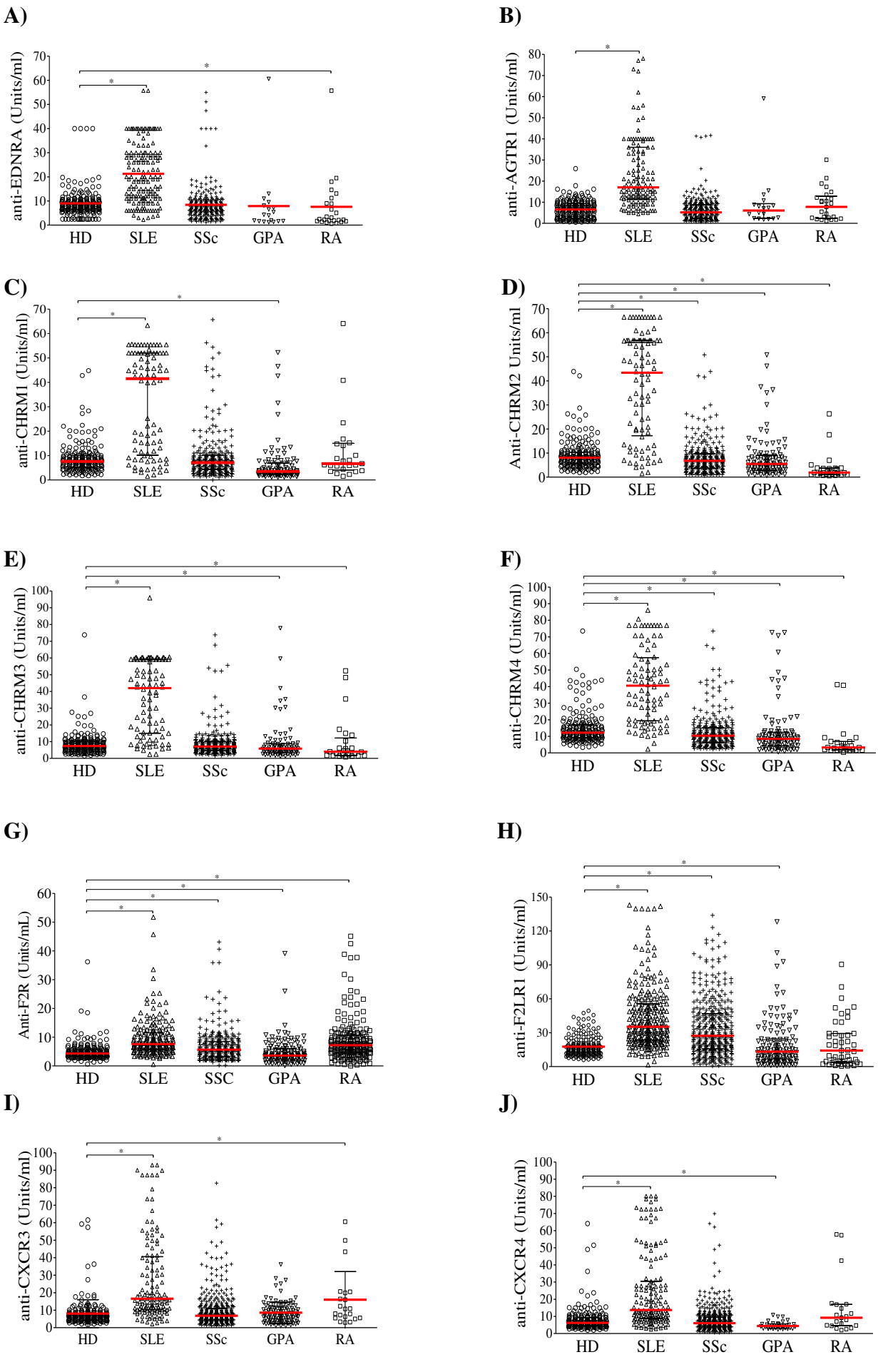

Supplementary Figure 1. Dysregulation of autoantibody concentrations in patients with autoimmune diseases. Graphics show concentrations of aab directed against **A-J**) 10 different GPCRs, comparing healthy donors (HD, n=197) to patients with autoimmune diseases. A total of 249 patients with systemic lupus erythematosus (SLE), 379 with systemic sclerosis (SSc), 128 with granulomatosis with polyangiitis (GPA), and 196 with rheumatoid arthritis (RA) were screened in this phase of the investigation. However, not all patients could be screened for the 10 aab due to sample limitation.

Supplementary Figure 2

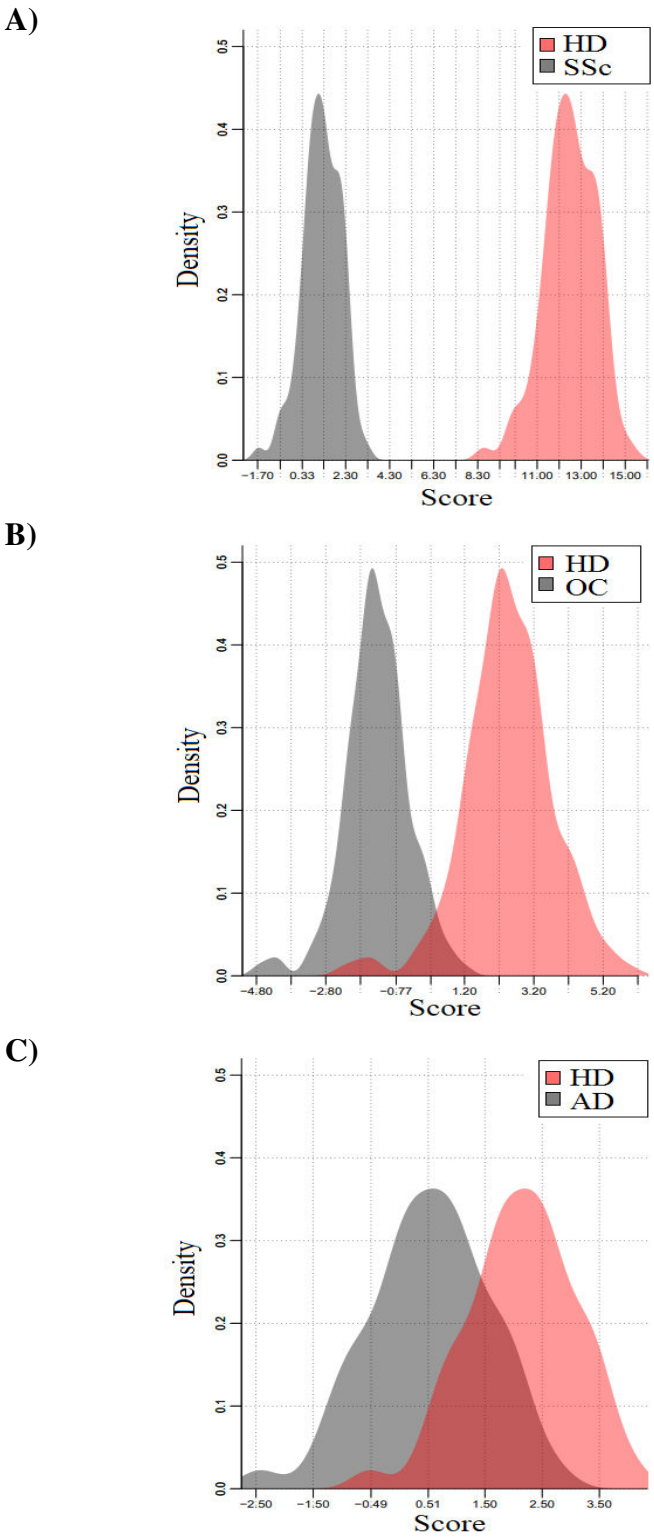

Supplementary Figure 2. **Linear discriminant analysis of autoantibody signatures differentiates healthy subjects and patients**. Density plots of the linear discriminating scores show the separation between individuals belonging to the disease groups compared to healthy donors (HD). **A**) HD *versus* patients with systemic sclerosis (SSc, **Supplementary Table 1,** *Cohort 1*; **Supplementary Table 2,** *aab dataset 1*, **B**) HD *versus* patients with ovarian cancer (OC, **Supplementary Table 1,** *Cohort 2*; **Supplementary Table 2,** *aab dataset 2*), and **C**) HD *versus* patients with Alzheimer's disease (AD, **Supplementary Table 1,** *Cohort 3*; **Supplementary Table 2,** *aab dataset 3*).

Supplementary Figure 3

A)

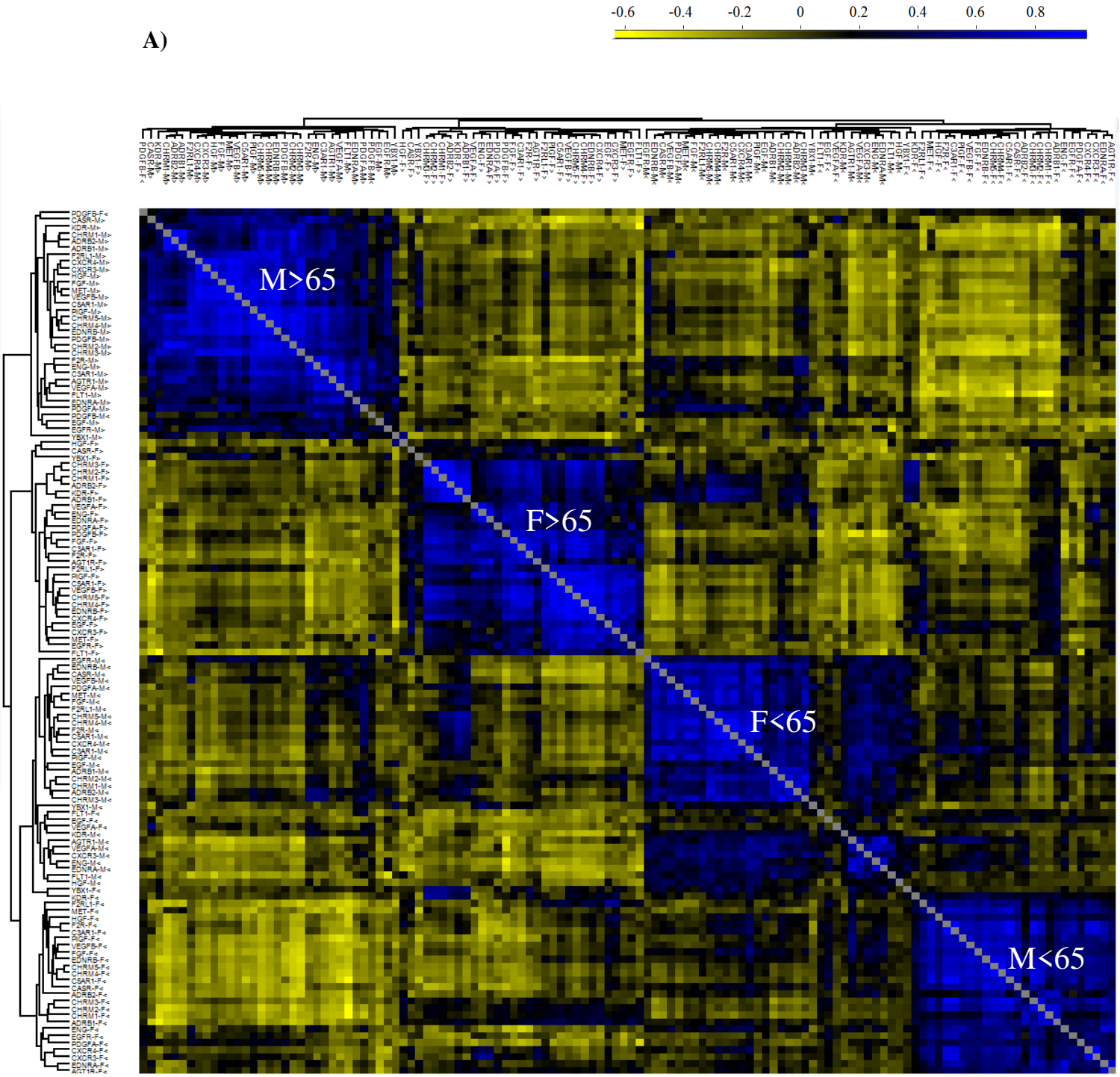

B)

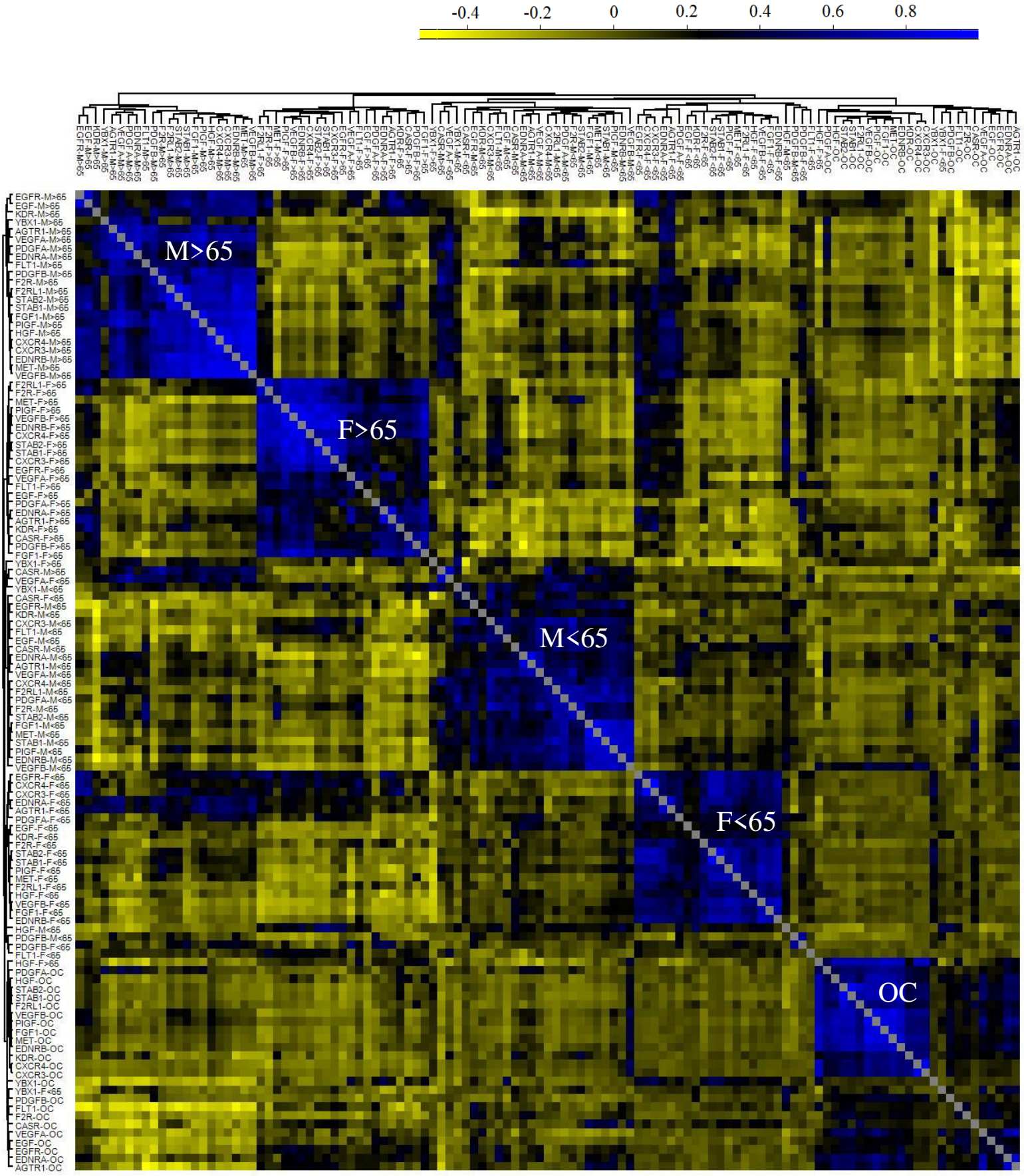

C)

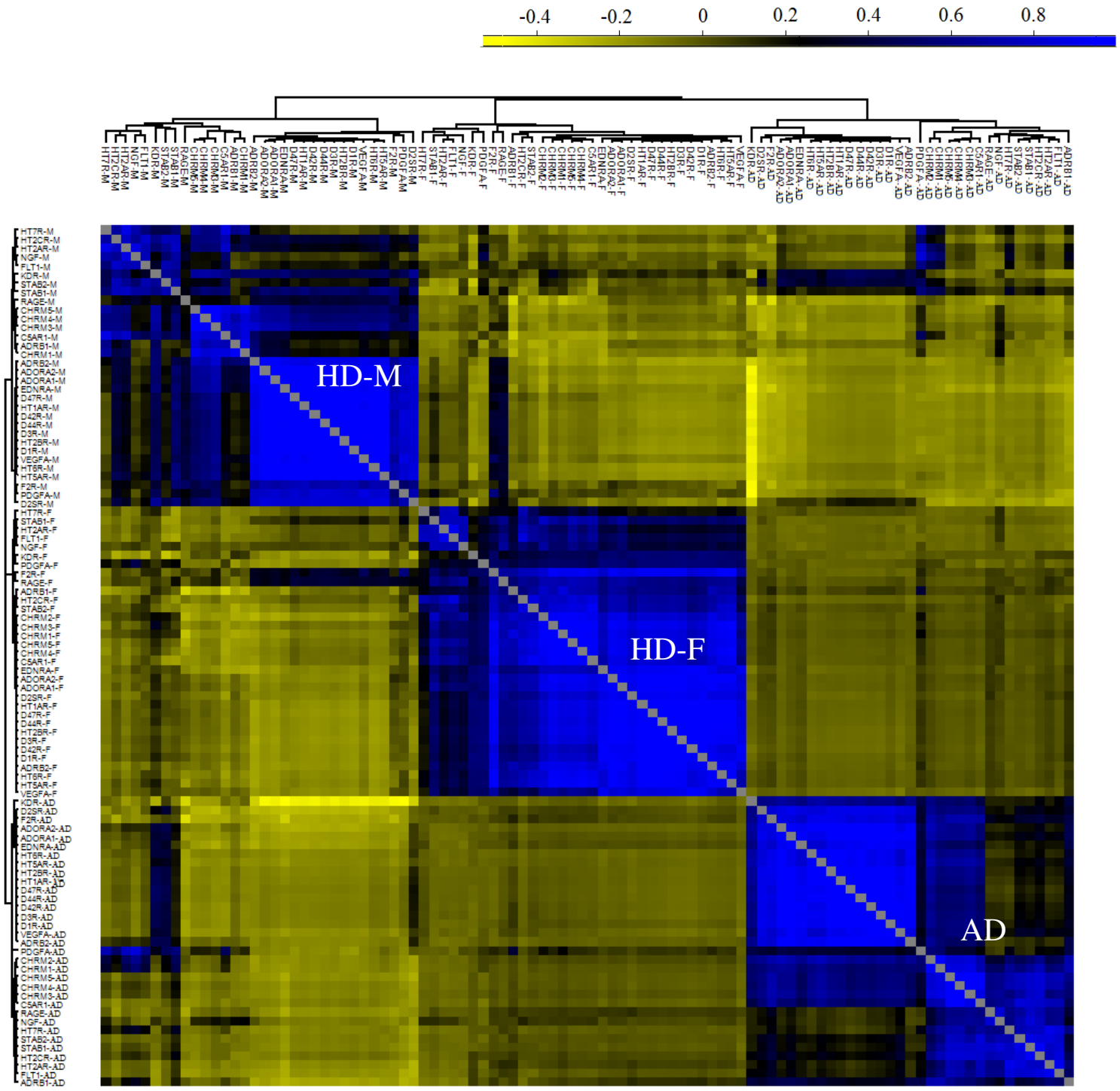

D)

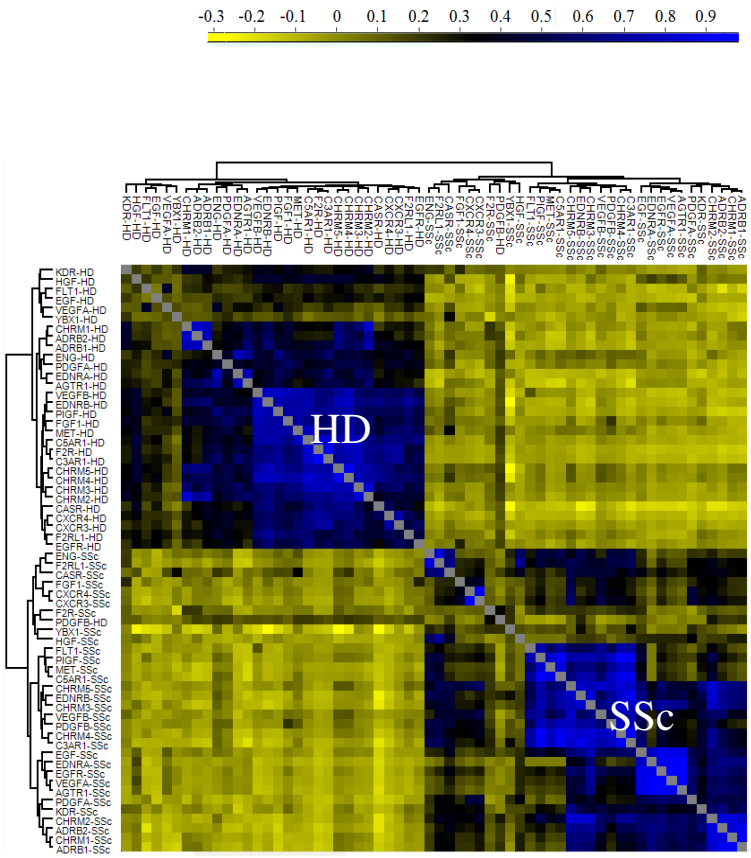
-0.3 -0.2 -0.1 0 0.1 0.2 0.3 0.4 0.5 0.6 0.7 0.8 0.9
HD
SSc

E)

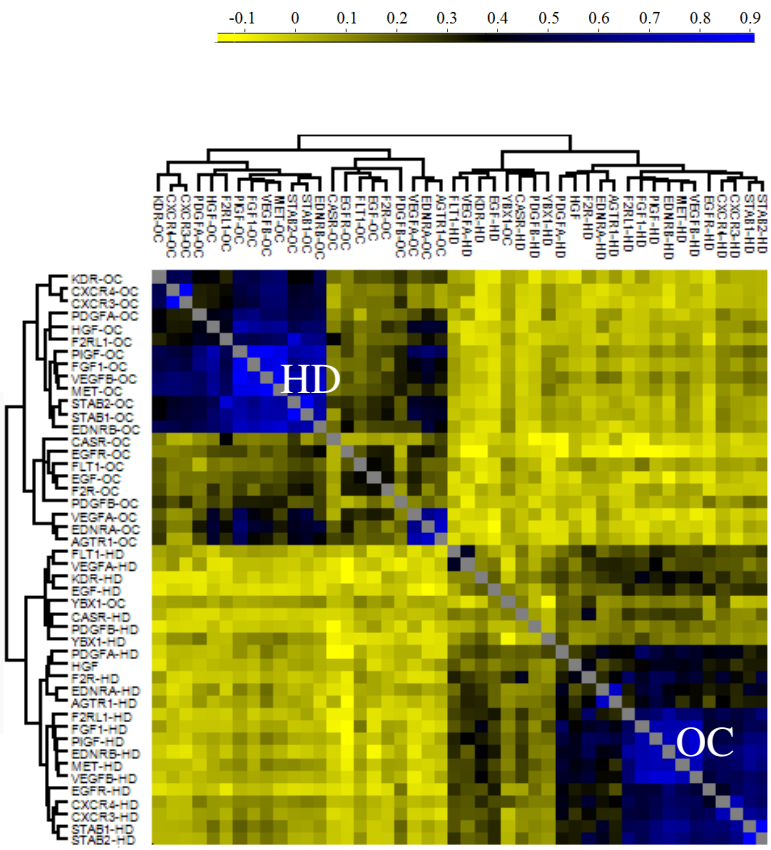
-0.1 0 0.1 0.2 0.3 0.4 0.5 0.6 0.7 0.8 0.9
HD
OC

F)

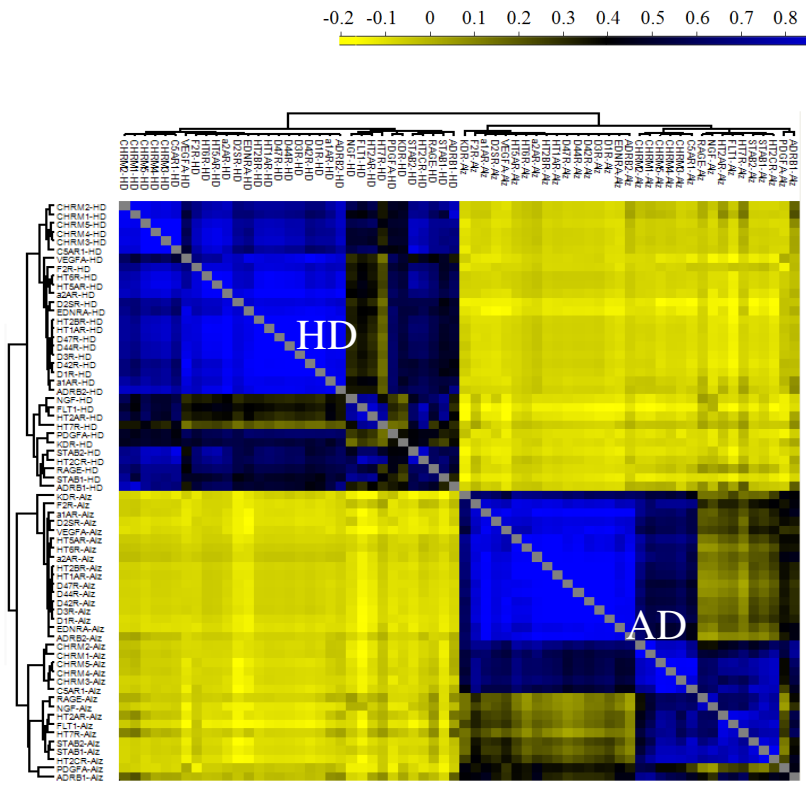
-0.2 -0.1 0 0.1 0.2 0.3 0.4 0.5 0.6 0.7 0.8 0.9
HD
AD

Supplementary Figure 3. Hierarchical clustering analysis reveals autoantibody correlation signatures according to gender, age and diseases. Correlogram matrices display clusters of aab**. A)** Heatmap displaying clusters of aab correlations from subgroups (females and males < and ≥ 65 years) of healthy donors (HD; **Supplementary Table 1,** *Cohort 1*; **Supplementary Table 2**, *aab dataset 1*). **B)** HD *versus* ovarian cancer **(**OC; **Supplementary Table 1,** *Cohort 2*; **Supplementary Table 2**, *aab dataset 2*). **C**) HD in relation to patients with Alzheimer's disease (AD, **Supplementary Table 1,** *Cohort 3*; **Supplementary Table 2**, *aab dataset 3*). The correlation matrices used to perform the hierarchical correlogram of OC and AD are provided as Source data. Due to the low number of healthy males < 65 years of age (HD Cohort 3), we only performed hierarchical clustering analysis of this group according to gender. **Supplementary table 1** provides further details about HD and patient groups. Analysis of non-subgrouped **D**) HD compared with systemic sclerosis (SSc), **E)** HD *versus* ovarian cancer **(**OC)**, F**) and HD in relation to patients with Alzheimer's disease (AD) are shown. Dendrograms on the top and the side of the correlation matrix display clusters of correlation between aab. The bar ranging from yellow to blue represents negative to positive correlations, respectively. In the heat map matrix, each small square represents pairwise correlation between aab.

Supplementary Figure 4

A)

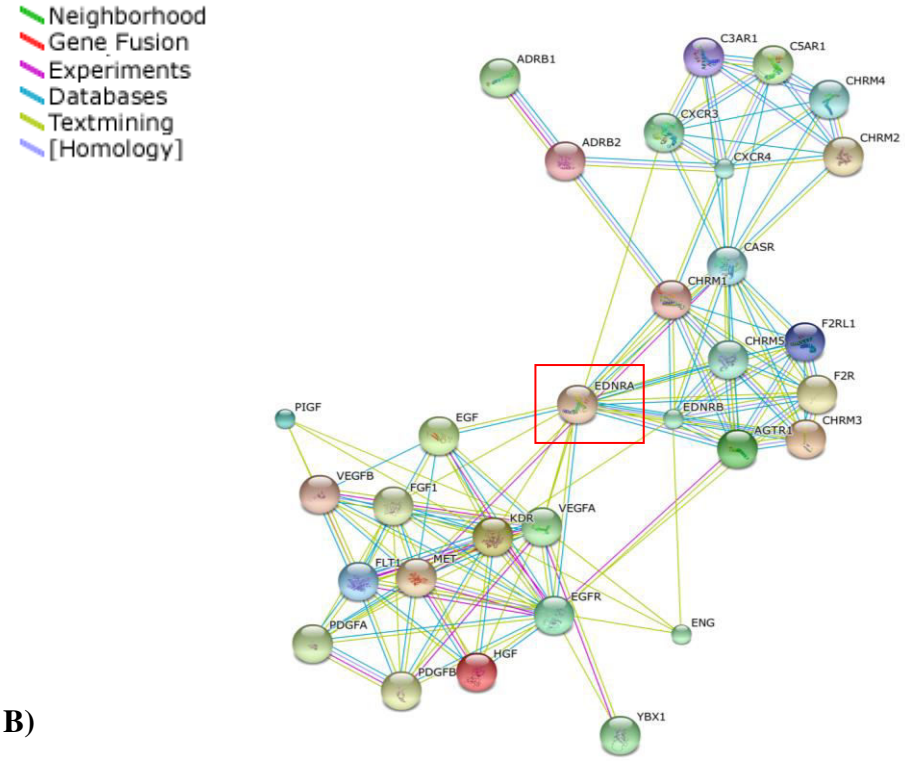

B)

GO Term	GO Biological Process	Molecules	p-value_FDR
GO:0030334	regulation of cell migration	VEGFA, HGFR, ENG, VEGFR1, CXCR3, PAR1, VEGFB, CXCR4, C3AR1, HGF, FGF1, EDNRA, VEGFR2, PDGFA, EGFR	1.26^{-12}
GO:0007200	phospholipase C-activating G-protein coupled receptor signaling pathway	M5, EDNRA, CASR, M1, M3, PAR1, M2, M4, AGTR1	1.26^{-12}
GO:0040017	positive regulation of locomotion	VEGFB, HGFR, CASR, VEGFR1, CXCR3, PAR1, C3AR1, HGF, FGF1, EDNRA , VEGFR2, PDGFA, EGFR	1.26^{-12}

Supplementary Figure 4. Network and gene ontology analysis of autoantibody targets. To help interpret the biological meaning of a putative physiological aab network we performed gene ontology analysis of aab targets (**Extended Data Tab 2,** *aab dataset 1*) using the STRING database. **A**) Different colored lines represent different forms of relationship evidences: red lines represent the presence of fusion evidence; green lines show neighborhood evidence; blue lines display co-occurrence evidence; purple lines exhibit experimental evidence; yellow lines demonstrate text mining evidence; and light blue lines display database evidence. The red frame indicates EDNRA in the center of the network. **B**) Lower panel lists physiologic functions regulated by interactions between GPCRs and growth factors or related signaling molecules. Enriched gene ontology (GO) biological processes were considered when false discovery rate (FDR) was less than 0.05.

A)

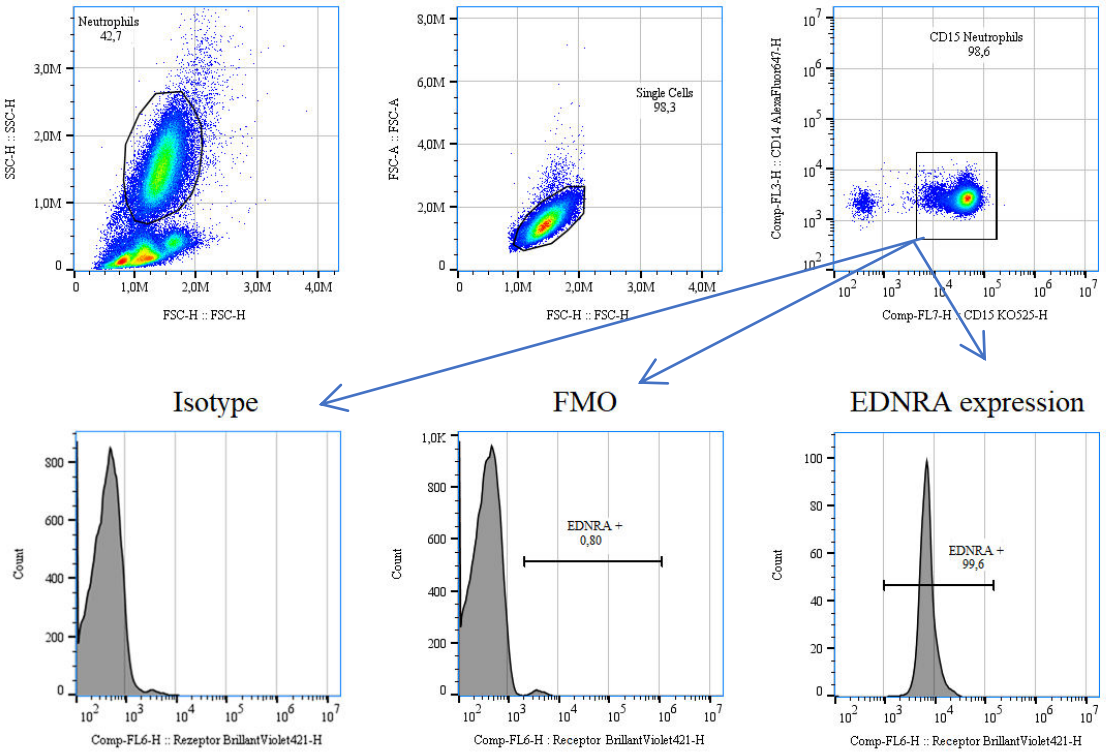

Supplementary Figure 5. Gating strategy for EDNRA expression. For MFI values an isotype control (Supplementary Table 3) was used to compensate for changes in the cytometry instrument sensitivity. Considering the multiple fluorochromes in the antibody panel to analyze EDNRA expression (**Supplementary Table 3**), the fluorescence minus one (FMO) control was determined when all the antibodies were present in the flow cytometry tube, except the antibody used to measure the EDNRA expression.

Supplementary Figure 6

A)

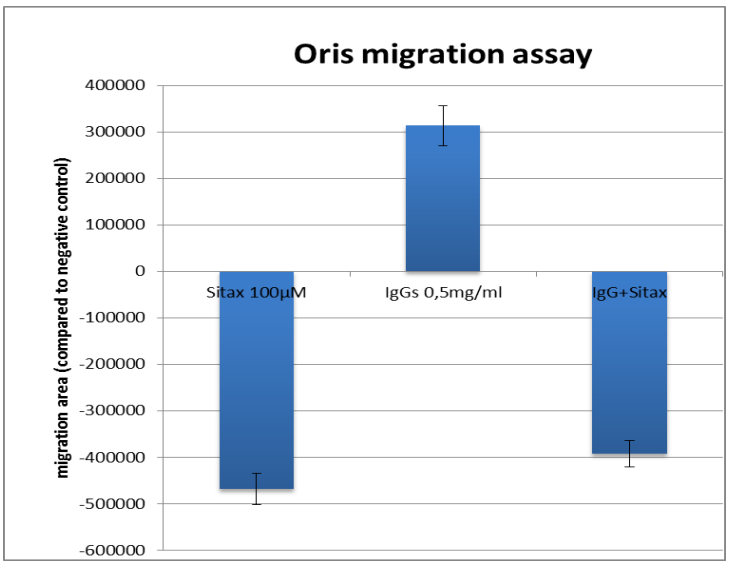

B)

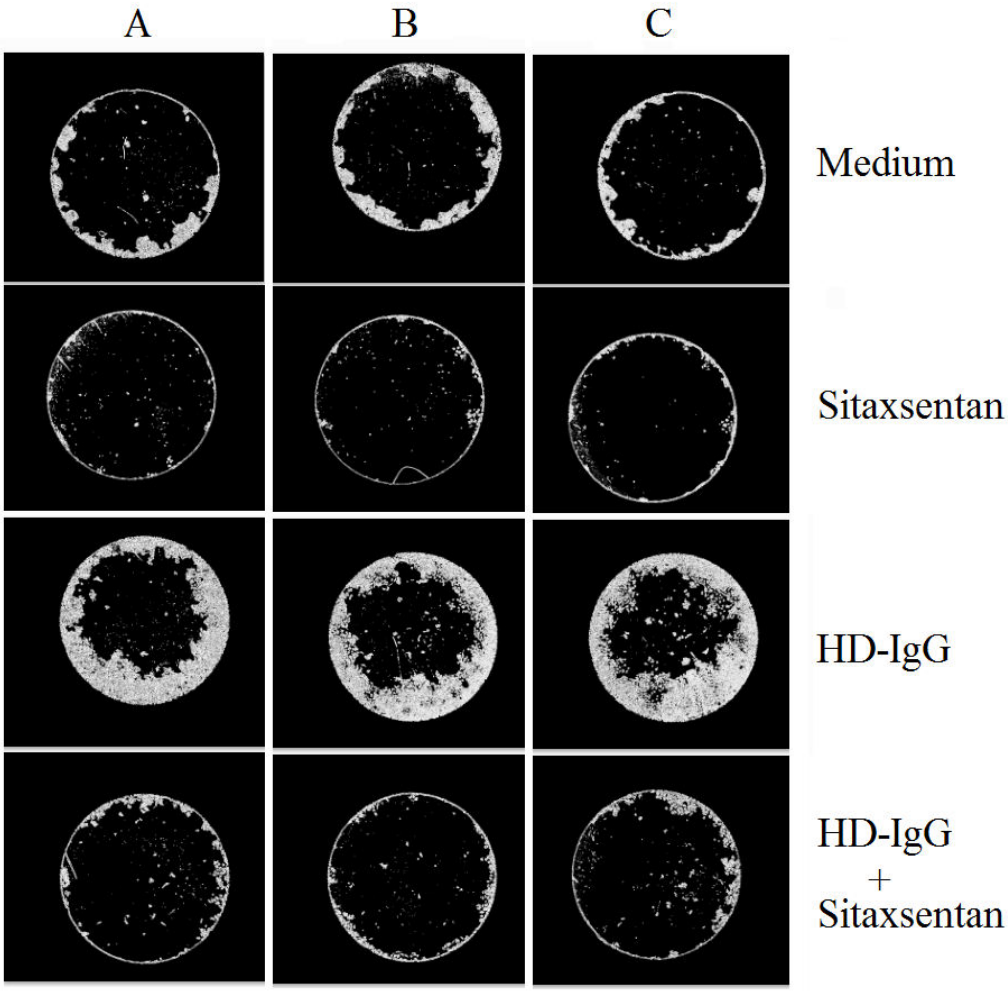

Supplementary Figure 6. Effect of HD-IgG on migration of the human pancreatic carcinoma Colo357 cell line. Chemotaxis of $3x10^5$ (cells/well) human pancreatic carcinoma Colo357 toward 0.5 mg/mL IgG from healthy donors (HD-IgG) was analyzed using Cell based Oris™ migration assay. **A)** migration area was determined by analysing **B)** migration images with the Fiji module of Image J software. Assays were performed in quadruplicates. One of three independent experiment is shown.

Supplementary Figure 7

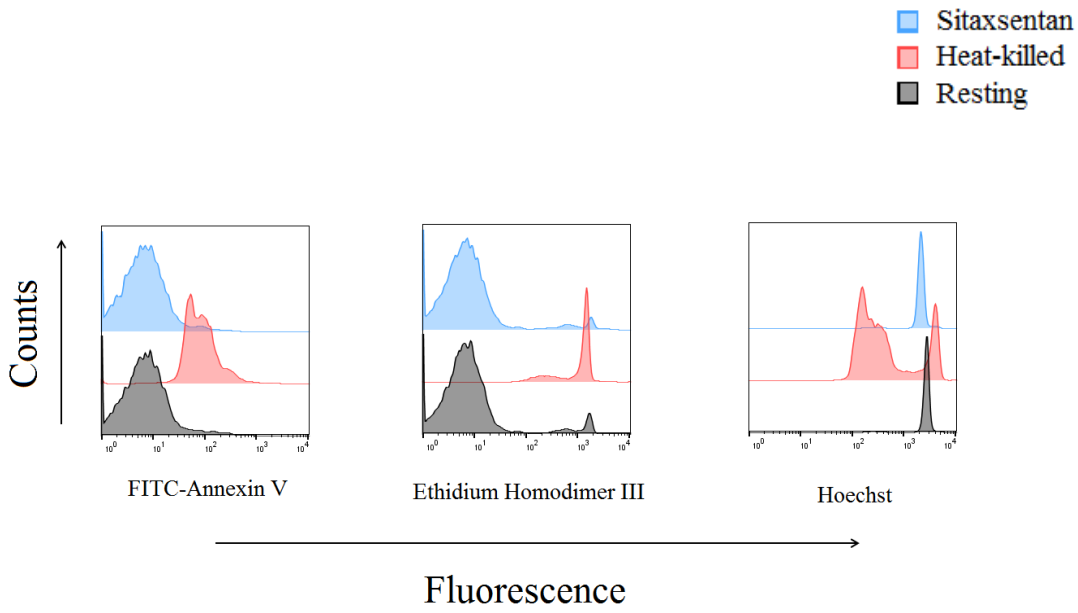

Supplementary Figure 7. Exposure to sitaxsentan, a potent endothelin receptor type A antagonist, has no toxic effect on neutrophils. Neutrophil apoptosis or necrosis was assessed by flow cytometric analysis. Left histogram displays the apoptotic cells stained by FITC-annexin V; middle histogram shows the necrotic cells stained by ethidium homodimer-III; right histogram demonstrates healthy donor cells stained by Hoechst. Heat-killed cells were used as experimental control. Results are representative of three independent experiments. The effect of sitaxsentan on neutrophil survival was analyzed by flow cytometry using the Apoptotic/Necrotic/Healthy Cells Detection Kit (PromoCell, Heidelberg, Germany) according to the manufacturer's instructions.

Supplementary Figure 8

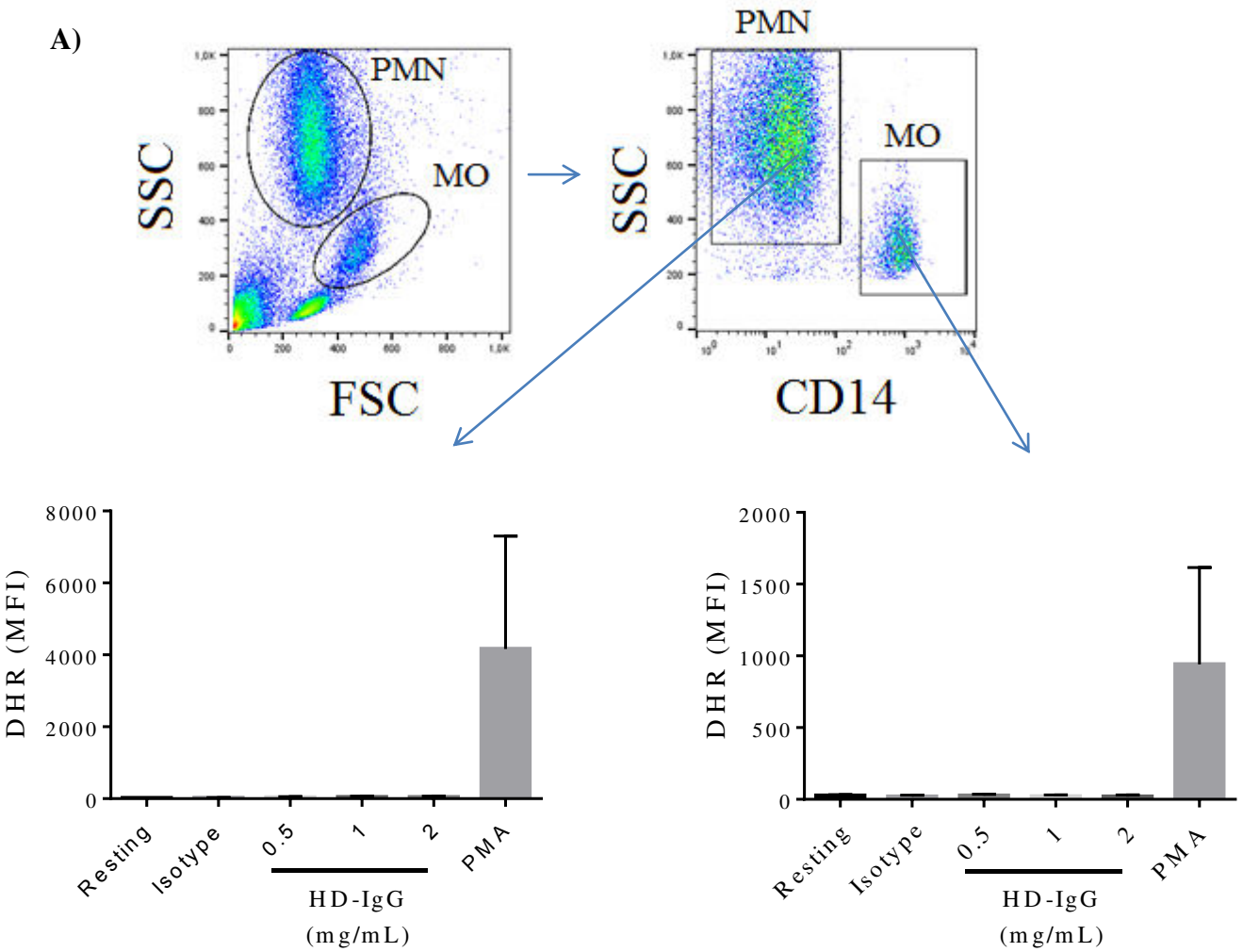

.

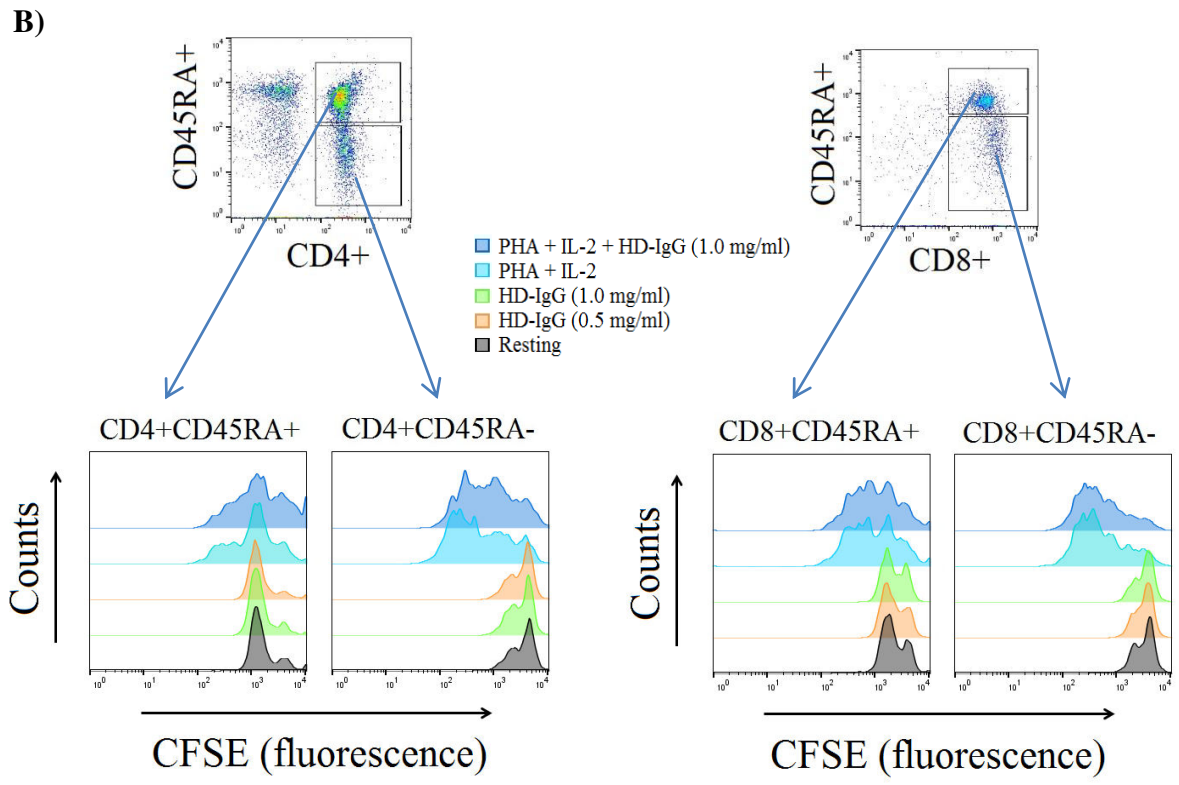

Supplementary Figure 8. Normal human IgG has no effect on respiratory burst of phagocytes and T cell proliferation (**A**) 300 ng/ml phorbol-12-myristate-13-acetate (PMA) but not 0.5 mg/mL healthy donor (HD)-IgG induces the respiratory burst of polymorphonuclear *neutrophils* (PMN) and monocytes (MO). White blood cells were stimulated *in vitro* in the presence of PMA for 60 min and analyzed by flow cytometry following 400 ng/ml dihydrorhodamine (DHR) 123 staining. Neutrophils and monocytes were gated according to size (forward scatter, FSC), granularity (side scatter, SSC) and pattern of CD14 expression. The median fluorescence intensity (MFI) of respiratory burst from three different experiments is shown. (**B**) PBMCs were isolated by Ficoll-Paque density gradient sedimentation. After 5 days at 37^{o}C in the absence or presence of 5 μg/ml phytohemagglutinin (PHA)/10 U/ml of IL-2 robust cell proliferation was observed, but, unaffected by HD-IgG (n = 3).

Supplementary Figure 9

A)

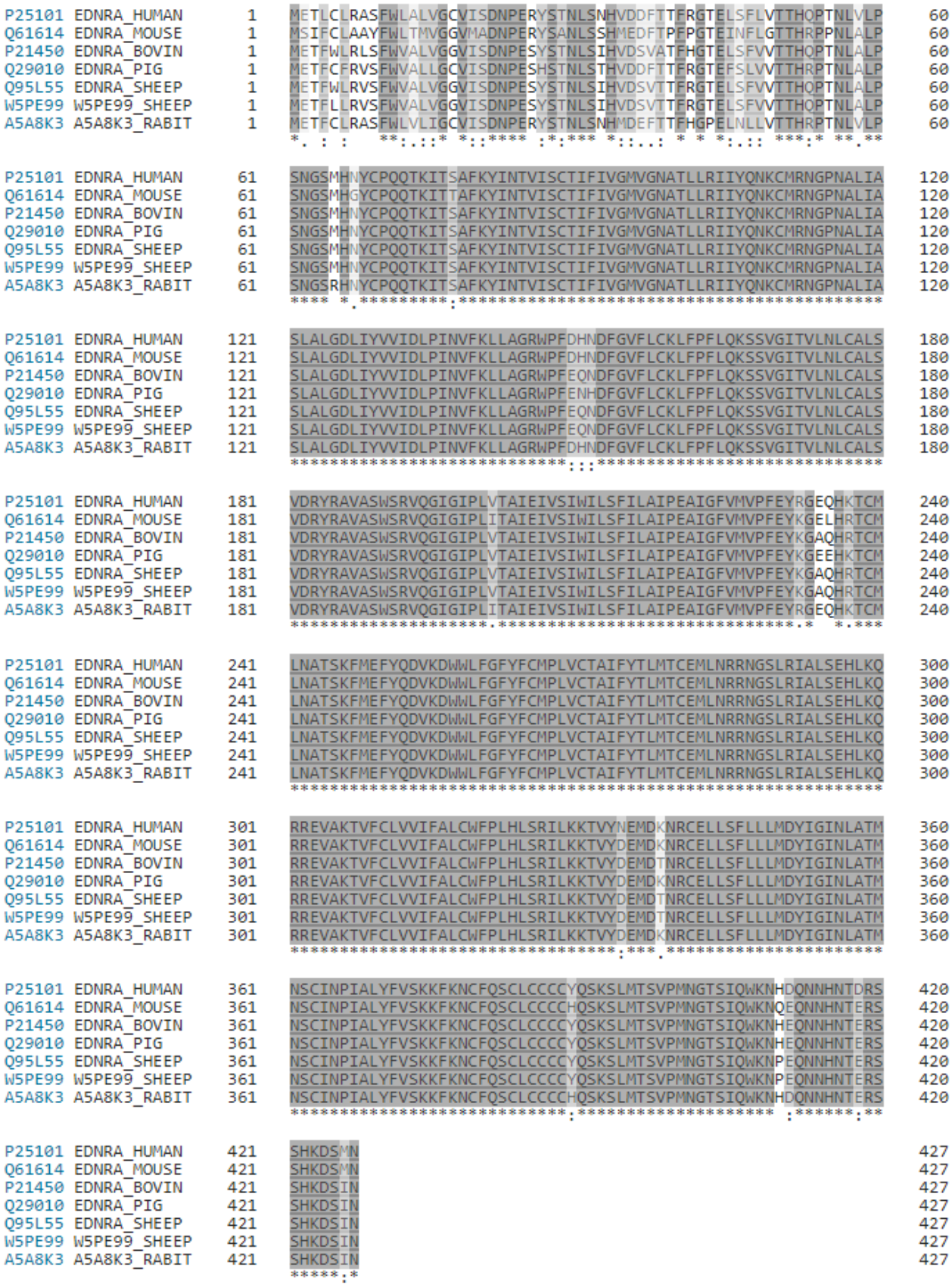

B)

```
P25101 EDNRA_HUMAN    1    METLCLRASFWLALVGCVISDNPERYSTNLSNHVDDFTTFRGTELSFLVTTHQPTNLVLP   60
Q61614 EDNRA_MOUSE    1    MSIFCLAAYFWLTMVGGVMADNPERYSANLSSHMEDFTPFPGTEINFLGTTHRPPNLALP   60
                           *. :** * ***::** *::*******:***.*::*** * ***:.** ***:* **.**

P25101 EDNRA_HUMAN   61    SNGSMHNYCPQQTKITSAFKYINTVISCTIFIVGMVGNATLLRIIYQNKCMRNGPNALIA  120
Q61614 EDNRA_MOUSE   61    SNGSMHGYCPQQTKITTAFKYINTVISCTIFIVGMVGNATLLRIIYQNKCMRNGPNALIA  120
                           ******.*********:*********************************************

P25101 EDNRA_HUMAN  121    SLALGDLIYVVIDLPINVFKLLAGRWPFDHNDFGVFLCKLFPFLQKSSVGITVLNLCALS  180
Q61614 EDNRA_MOUSE  121    SLALGDLIYVVIDLPINVFKLLAGRWPFDHNDFGVFLCKLFPFLQKSSVGITVLNLCALS  180
                           ************************************************************

P25101 EDNRA_HUMAN  181    VDRYRAVASWSRVQGIGIPLVTAIEIVSIWILSFILAIPEAIGFVMVPFEYRGEQHKTCM  240
Q61614 EDNRA_MOUSE  181    VDRYRAVASWSRVQGIGIPLITAIEIVSIWILSFILAIPEAIGFVMVPFEYKGELHRTCM  240
                           ******************:*****************************:** *:***

P25101 EDNRA_HUMAN  241    LNATSKFMEFYQDVKDWWLFGFYFCMPLVCTAIFYTLMTCEMLNRRNGSLRIALSEHLKQ  300
Q61614 EDNRA_MOUSE  241    LNATSKFMEFYQDVKDWWLFGFYFCMPLVCTAIFYTLMTCEMLNRRNGSLRIALSEHLKQ  300
                           ************************************************************

P25101 EDNRA_HUMAN  301    RREVAKTVFCLVVIFALCWFPLHLSRILKKTVYNEMDKNRCELLSFLLLMDYIGINLATM  360
Q61614 EDNRA_MOUSE  301    RREVAKTVFCLVVIFALCWFPLHLSRILKKTVYDEMDKNRCELLSFLLLMDYIGINLATM  360
                           *********************************:**************************

P25101 EDNRA_HUMAN  361    NSCINPIALYFVSKKFKNCFQSCLCCCCYQSKSLMTSVPMNGTSIQWKNHDQNNHNTDRS  420
Q61614 EDNRA_MOUSE  361    NSCINPIALYFVSKKFKNCFQSCLCCCCHQSKSLMTSVPMNGTSIQWKNQEQNNHNTERS  420
                           ****************************:*******************::******:**

P25101 EDNRA_HUMAN  421    SHKDSMN                                                      427
Q61614 EDNRA_MOUSE  421    SHKDSMN                                                      427
                           *******
```

Supplementary Figure 9. Sequence alignment of endothelin receptor type A. A) A multiple sequence alignment of endothelin receptor type A (EDNRA) show high conservation (87.58% identical) among different species and between **B)** *Homo sapiens* and *Mus musculus* (92.27% identical). Alignment of EDNRA was performed using Clustal Omega program (https://www.uniprot.org/align/) and EDNRA UniProt identifiers.